Contrib. Mineral. Petrol. 59, 41 – 93 (1976)

Contributions to Mineralogy and Petrology

Shock Processes in Porous Quartzite: Transmission Electron Microscope Observations and Theory

Susan Werner Kieffer, Prem P. Phakey,* and John M. Christie

Department of Geology and Institute of Geophysics and Planetary Physics, University of California, Los Angeles, California 90024, USA

Abstract. A high-resolution study of shocked Coconino Sandstone from Meteor Crater, Arizona, was undertaken using transmission electron microscopy to investigate the textural relations of high-pressure phases produced by meteorite impact. In weakly shocked rocks (estimated average pressure, $\bar{P} < 100$ kb), quartz in the interiors of grains retains its initial microstructure, but near original grain boundaries, quartz is altered by fractures and planar features resembling Brazil twins, and is partially transformed to coesite and glass. In moderately shocked rocks (estimated average pressure, $100 < \bar{P} < 250$ kb), as much as 50% of the residual quartz is fractured but otherwise undeformed. Near grain boundaries relatively undamaged quartz exists in direct contact with coesite and stishovite. Filamentary, microvesicular "froth" fills cracks and fractures in the regions containing high-pressure phases. Coesite present in regions which are collapsed pores has a unique texture, not previously reported for a shock-formed phase: the grains are equidimensional and form a mosaic pattern characteristic of products of high-temperature recrystallization. In strongly shocked rocks (estimated pressure $\bar{P} < 250$ kb) quartz contains abundant glass lamellae, identical to optical "planar features" except that they are so closely spaced that they would not be resolved optically. Vesicular glassy regions in strongly shocked rocks contain remnants of large (~ 5 μm) coesite crystals, indicating that the shock-formed glass in these regions formed by melting of coesite rather than quartz.

The textural relationships of coesite, stishovite and glass observed in these rocks provide evidence regarding the processes of the formation and destruction of high pressure phases during the passage of a shock wave. Three types of coesite are observed: (1) Polycrystalline coesite which formed directly from quartz grains, perhaps with topotactic control; (2) Single-crystal coesite grains which have partially inverted to form thetomorphic coesite glass; (3) Well-equilibrated coesite which nucleated and grew from a hot precursor phase, believed to be amorphous silica with silicon in six-fold

* Permanent address: Department of Physics, Monash University, Clayton, Victoria, Australia

coordination. The texture of the stishovite, found only in the moderately shocked rocks, leads us to conclude that it formed by direct nucleation and growth from quartz grains. We believe that only a small amount of stishovite was formed and that the stishovite which was formed did not invert to glass. Three types of glass are observed: (1) Thetomorphic coesite and quartz glass, formed by the inversion of the crystalline phases; (2) Glass (lechatelierite) pervaded with relatively large spheroidal vesicles and schlieren, generally formed by melting of coesite crystals; (3) Glass ("froth") pervaded with vesicles of irregular, generally nonspheroidal shape, having diameters of tens of Angstroms, formed by the interaction of quartz, coesite or glass with hot water vapor.

A detailed description of the reaction of porous sandstone to the passage of shock waves of milliseconds duration is derived and shock Hugoniot data for single crystal quartz, water, and wet and dry rocks are reviewed in order to provide pressure estimates for each type of rock and to provide a basis for comparing naturally shocked samples with laboratory data. In weakly shocked rocks, pore closure is accomplished by brittle fracture of grains and rotation of fragments into pores. In moderately and strongly shocked rocks, pore closure is accomplished by *jetting*, the extrusion of molten streams of hot material into the pores, forming cores of extremely hot material from which the well-equilibrated coesite aggregates crystallized. In the moderately shocked rocks, these coesite crystals are preserved within the cores. In strongly shocked rocks, most of the coesite melts to form lechatelierite.

The history of water contained within pores during passage of a shock wave is complex. In moderately shocked rocks, hot steam forms and reacts with quartz, coesite and stishovite in the vicinity of the collapsed pores. The hot steam erodes grains in some places, forming a silica-rich fluid which can subsequently be deposited in other places in the rocks. In strongly shocked rocks, silica and hot water intermix to form a super-critical SiO_2-H_2O solution, from which the water exsolves late in the rarefaction event to form vesicular glass.

1. Introduction

To interpret the record of meteorite impacts on a planetary surface and to interpret many current laboratory shock experiments of geophysical importance, it is necessary to relate effects produced by the passage of a shock wave to the initial state of the material and to the pressure, temperature, and duration of the shocks to which the material has been subjected. In the present paper we give the results of a transmission electron microscope (TEM) study of the occurrence and origin of high-pressure phases in naturally shocked Coconino Sandstone from Meteor Crater, Arizona. This is the first set of extensive submicroscopic observations on shocked rocks to be reported. Systematic studies of the occurrence and textural relationships of high-pressure phases may provide data for formulating a theory of the behavior of minerals which undergo phase

changes under shock conditions. Because shock wave and hydrostatic equation-of-state are available from laboratory studies on quartz, we feel that a study of the Coconino quartzite at Meteor Crater affords a unique opportunity to relate naturally occurring shock products to conditions of pressure and temperature measured in the laboratory.

The Coconino Sandstone is a nearly pure quartzite, and the shocked samples found at Meteor Crater are products of a variety of pressure and temperature conditions which occurred during a natural impact event. Numerous studies of the geology and petrography of the rocks at Meteor Crater have contributed to a substantial understanding of impact processes and products. Shoemaker (1960, 1963) described the occurrence and distribution of shocked rocks around the crater and provided the model for impact penetration mechanics which forms the general basis for interpretation of the shock history of terrestrial and lunar impact craters. Chao and others (1960, 1962) first discovered naturally occurring coesite and stishovite in dense, platy Coconino Sandstone specimens, and Chao (1967) has related the occurrence of the high-pressure phases to shock features in the deformed quartz grains. A study of the Coconino Sandstone by techniques of optical microscopy and single-crystal and quantitative X-ray diffraction by Kieffer (1970, 1971) has led to systematic classification of the shocked rocks and to a model for formation of high-pressure phases in porous media under shock conditions.

2. Background and Purpose of Work

The unshocked Coconino Sandstone, as exposed at Meteor Crater, is a pale buff, white, or pink cross-bedded quartzite of average porosity 10 to 20%. In hand specimen the rocks may be either laminated or massive (Kieffer, 1971). Detrital quartz grains in the sandstone are generally well rounded, and, in the massive rocks have longest dimensions between 0.1 mm and 3.9 mm, with a mean length of 0.2 mm (Fig. 1a). The shocked samples may be divided into five classes arranged in order of decreasing quartz content (Fig. 1b). The composition of the rocks in these classes is:

Class 1. Weakly shocked rocks containing no high-pressure phases and 95% or more quartz: (a) with petrographically observable remnant porosity; (b) without petrographically observable remnant porosity.

Class 2. Moderately shocked rocks containing 80 to 95% quartz. These rocks typically have 2 to 5% coesite, 3 to 10% glass, and no detectable amount of stishovite.

Class 3. Moderately shocked rocks containing 45 to 80% quartz. These rocks typically have 18 to 32% coesite, trace amounts of stishovite, and 0 to 20% glass.

Class 4. Strongly shocked rocks containing 15 to 45% quartz. These rocks typically have 10 to 30% coesite, 20 to 75% glass, and no detectable stishovite.

Class 5. Very strongly shocked rocks that contain 0 to 15% quartz. These rocks may have 0 to 5% coesite, 80 to 100% glass, and no detectable stishovite.

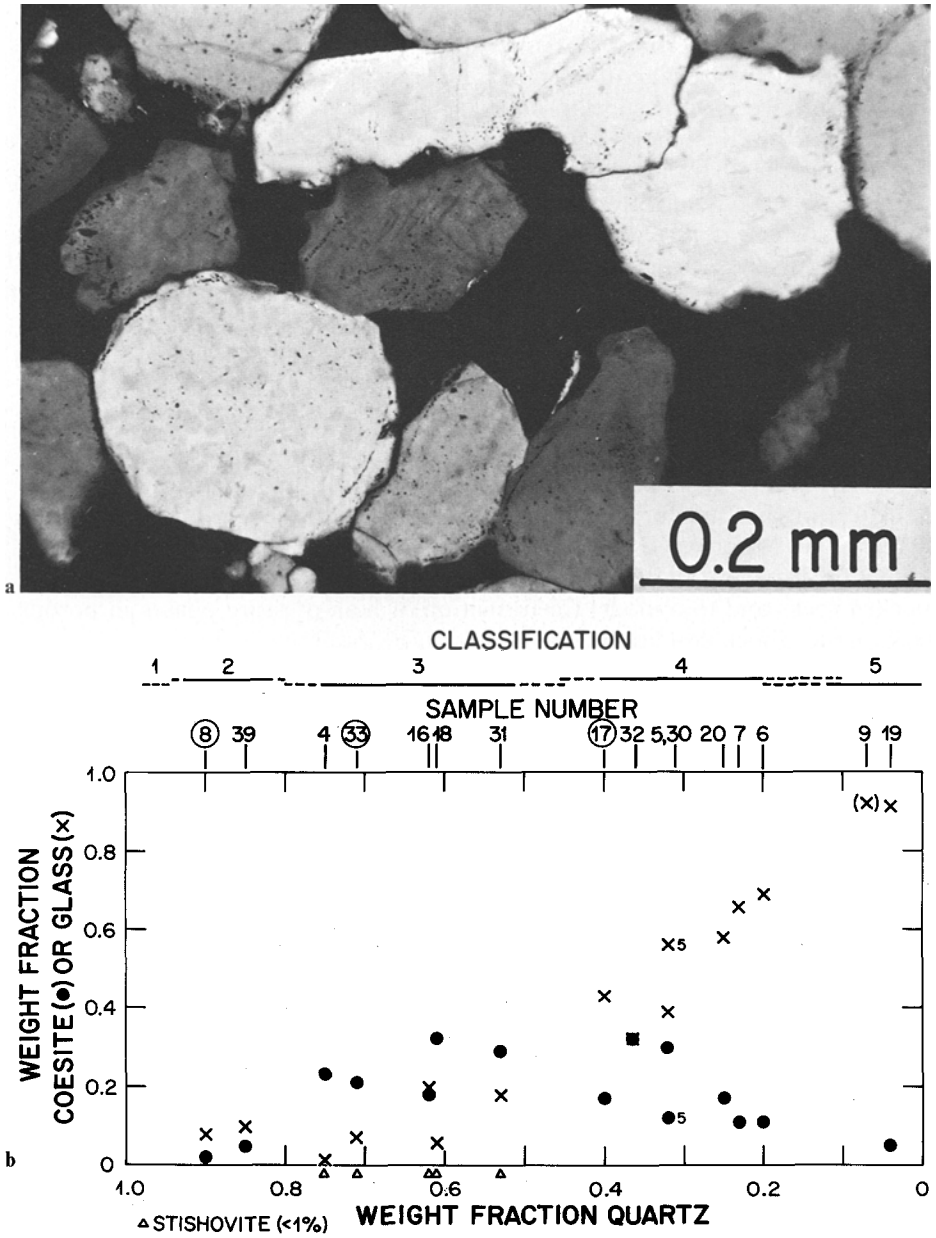

Fig. 1. a Photomicrographs of "unshocked" Coconino Sandstone obtained from the "silica pits" on the south rim of Meteor Crater; crossed polarizers. Boundaries between original detrital quartz and recrystallized quartz cement are frequently marked by lines of vesicles. **b** Abundance of coesite (●) and glass (×) in shocked Coconino Sandstone, as a function of quartz content. Rocks in which stishovite is detectable by X-ray methods (i.e., content is greater than 0.25 percent by weight) are indicated by a triangle below the abscissa. Limiting quartz contents of the five classes of rocks and sample numbers are shown on the top line. Sample numbers of rocks used in this TEM study are circled

Rock fabric and texture are strongly correlated with this mineralogical classification.

Values of mass fraction obtained by X-ray diffraction have a standard deviation of less than 10 percent for quartz and less than 6 percent for coesite (Kieffer, 1970). The glass content is obtained by subtracting the quartz plus coesite content from 100 percent. Sine the rocks may contain to 5 percent minerals other than SiO_2, all glass values contain an additional uncertainty. It should also be remembered that X-ray techniques are limited to detecting crystals larger than 500 Å to 1,000 Å and that crystals smaller than this will be considered "amorphous" in such an analysis. A discussion of the effect of particle size on X-ray line intensity is given in Kieffer (1970).

Because of the length of the descriptions of new observations presented here, we do not review the previous optical and X-ray work done by Kieffer (1971) on these rocks. The reader is referred to that paper for information on (1) the petrography of unshocked Coconino Sandstone, (2) the system of classification of the shocked Sandstones, (3) the petrographic textures of the shocked Sandstone, and (4) the detailed shock history of the samples as dedeced from optical microscope observations.

3. Method of Study

Sample Preparation

For TEM observations a rock sample of each of Classes 2, 3, and 4 (Fig. 2) was selected on the basis of characteristic composition, hand specimen features, and petrographic features in thin section. (Class 1 rocks were not studied because they do not contain resolvable amounts of high-pressure phases; a discussion of Class 1 rocks and weak shock wave propagation is given in Kieffer, 1975a. Class 5 rocks were not studied because they resemble Class 4 rocks except that they are nearly all glass.) A thin section of each sample, polished on both sides, was prepared. Because of the systematic occurrence of the SiO_2 phases in these rocks it is possible to select under the optical microscope regions of dimensions on the order of 100 μm which contain the high-pressure phases (Kieffer, 1971). Cores of approximately 3 mm diameter, containing as many of these regions as possible, were drilled from the thin section with an ultrasonic coring drill. A copper electron microscope grid (75 mesh) was glued to one side, and a copper support ring was affixed around the circumference on the opposite side. The sample, thus supported, was placed in an ion thinning specimen holder (Heuer et al., 1971) and was thinned in a Commonwealth Scientific Ion Milling Machine for 10 to 20 h until a small perforation appeared in the area of interest. The sample was rephotographed at this point so that accurate correlation could be made with regions in the original optical thin section. During TEM observations, the locations of electron micrographs with respect to the optical micrographs were obtained by means of "shadowgraphs" taken at optical magnifications in the electron microscope. A JEM 120 electron microscope operated at 120 kv was used for this study.

Though the problem of identification of the submicroscopic phases in these shocked rocks is particularly well suited for transmission electron microscopy, the problems of sample preparation were more exacting than usual for singe phase crystals or aggregates. Because of the extreme heterogeneity of many of the rocks on microscopic scale, it was necessary to follow the progress of ion thinning in great detail, with repeated photographs, to be sure that the areas desired were examined in the electron microscope. Moreover, although the rocks consist almost entirely of SiO_2, up to four phases (glass, quartz, coesite, and stishovite) are present, and these thin at markedly different rates in the ion beam (at rates decreasing with increasing density). Consequently, the regions containing the dense phases were only sufficiently thin when much of the glass and quartz

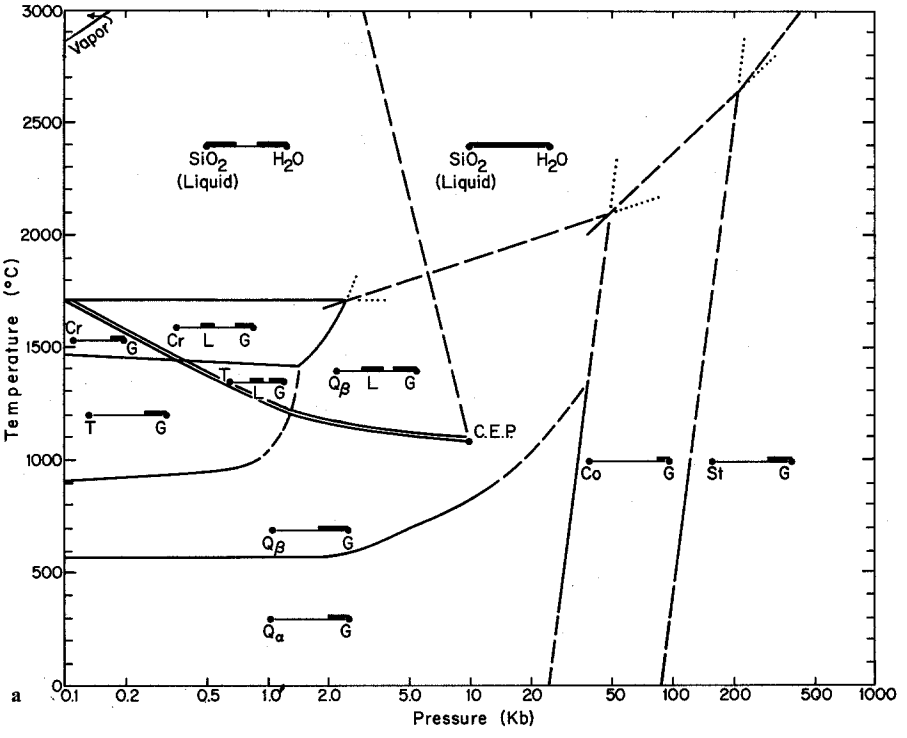

a

Comparison of Polycrystalline Diffraction Patterns for SiO_2

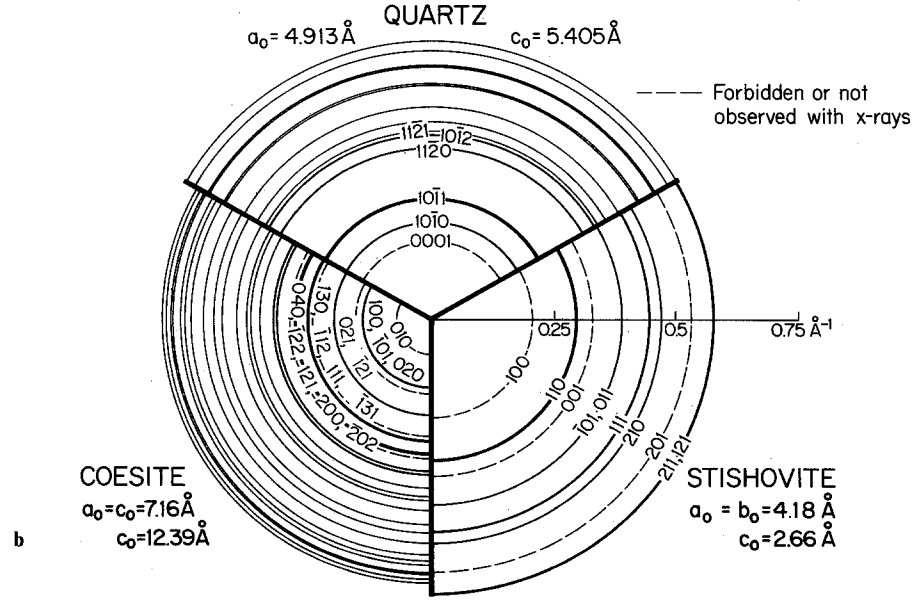

b

had been removed, giving problems of mechanical stability of the samples, and only very limited areas of the "foils" were electron transparent in the complex polyphase regions. Thus, the quality of the foils was notably inferior to that generally obtained with single-phase mineral specimens of coarser polyphase aggregates.

Phases of SiO_2 and Their Identification

Four phases of SiO_2 have been identified in shocked Coconino Sandstone: quartz, coesite, stishovite and glass. The stability fields of these phases under dry and wet conditions are shown in Figure 2a.

Quartz, the stable form of SiO_2 under ordinary conditions, exists in the trigonal α-quartz structure ($P3_121$, $P3_221$) below 573° C. For indexing the diffraction patterns we have used *d*-spacings based on the unit cell $a_0 = 4.913$ Å, $c_0 = 5.405$ Å at 25°C (Frondel, 1962). The density was assumed to be 2.65 g/cm^3.

Coesite (Coes, 1953), a monolinic phase of SiO_2 with silicon tetrahedrally coordinated to four oxygen atoms, is stable at room temperature in the approximate range 30 to 70 kb (Fig. 2a). For indexing diffraction patterns we have used *d*-spacings based on the setting (C2/c) (Ramsdell, 1955) with a = 7.16 Å, b = 12.39 Å, and c = 7.16 Å, and with a density of 2.94 g/cm^2. The angle β equals 120°, giving the structure pseudohexagonal symmetry.

Stishovite (Stishov and Popova, 1961), the densest phase of SiO_2, has silicon in six-fold coordination and is stable above approximately 70 kb at room temperature (Fig. 2a). Stishov and Below (1962) assigned stishovite the primitive tetragonal cell of rutile ($D_{4h}^{14} = P4_2/mnm$), with a = 4.18 Å, c = 2.66 Å, and found a density of 4.35 g/cm^3 for synthetic stishovite. We used these unit cell dimensions to obtain our reference *d*-spacings.

The calculated polycrystalline diffraction patterns for quartz, coesite, and stishovite are shown in Figure 2b. The X-ray intensities of the various lines are shown schematically in the figure; these were found to be a useful indicator of the electron diffraction intensities in extremely fine-grained polycrystalline areas. In addition to quartz, coesite, and stishovite – all identified – cristobalite, tridymite, and keatite were considered as possible phases, but were not detected in any of the regions examined. Glass is easily identified in the electron microscope because it does not diffract electrons and its contrast does not change on tilting the sample.

The diameter of the smallest selected area aperture used to obtain electron diffraction patterns was 1 μm. It is nearly impossible to identify SiO_2 phases by *d*-values alone if the polymorphs are intermixed on a scale appreciably less than the diameter of the aperture because of the similarities in diffraction patterns, evident from the "bullseye" in Figure 2b. It is possible to identify coesite uniquely by the poorly resolved doublet (040, $\bar{1}22$, 200 and 012, $\bar{2}12$) at 3.090 and 3.007 Å, and by the frequently observed presence of the (100, $\bar{1}01$ and 020) "forbidden" lines at 6.2 Å, but it is difficult to identify quartz if coesite is present because of the similarity of *d*-values of the strongly diffracting planes. (Diffraction spots or lines in polycrystal diffraction patterns that are "forbidden", because of systematic space-group extinctions, may be present in electron diffraction patterns because of the phenomenon of *double diffraction*.) Similarly, stishovite is undetectable in the presence of coesite and is difficult to detect in the presence of quartz. Because of these ambiguities we generally attempted to place the selected area aperture for diffraction patterns on a part of the material which appeared to be a single phase or a single crystalline phase mixed with glass, which gives only diffuse and weak "glass rings" in the diffraction pattern.

Fig. 2. a Phase diagram of the system SiO_2 and SiO_2-H_2O based on data from Ostrovsky (1966), Kennedy et al. (1962), and Takahashi (1963). The symbols have the following meanings: Q_α, alpha quartz; Q_β, beta quartz; *T*, tridymite; *Cr*, cristobalite; *Co*, coesite; *St*, stishovite; *L*, liquid; *G*, vapor; *C.E.P.*, critical end point of the upper three phase region. The lower three-phase region is not shown. Phase boundaries in the range of measured data are shown in solid lines; extrapolated boundaries are dashed; metastable extensions used to extrapolate phase lines are dotted. The melting curve of wet SiO_2 is shown in double thickness. The melting curves of coesite and stishovite were estimated from the Clausius-Clapeyron equation. The bars show schematically the degree of mixing of end members into the various phases. **b** Polycrystalline electron diffraction rings expected for SiO_2 polymorphs calculated from X-ray data. Dashed rings correspond to forbidden lines, which are frequently observed on electron diffraction patterns due to double diffraction

For calibration, electron micrographs and electron diffraction patterns were obtained on coesite and stishovite chemically extracted from the shocked Coconino Sandstone by E.C.T. Chao and by Kieffer. In general, recovered coesite and stishovite particles are much larger than the material we observed in situ, probably because smaller particles are lost in the hydrofluoric acid recovery procedure. Therefore, although the recovered particles provided excellent diffraction patterns which we used for calibration, the grain morphologies of recovered coesite and stishovite do not prove of much value in identification of these phases in situ.

4. Class 2 Rocks

Petrographic Description

A well-indurated, dense, white rock (No. 8 in Fig. 1b) with closely spaced ($\sim$0.5 mm), subparallel fractures was selected as a characteristic Class 2 rock for this study. This rock was initially $2.5 \times 2.5 \times 5$ cm and was obtained from mixed debris in the bottom of Meteor Crater (see Kieffer, 1971, Fig. 1 for a geologic map of Meteor Crater with sampling localities identified). The subparallel fractures on the hand specimen are apparently extension fractures because in thin section displacements of individual grains parallel to the fractures generally cannot be detected.

The composition of this rock (after removal of 6 percent calcite deposited during post-cratering weathering) was determined from quantitative X-ray diffraction studies to be 90 percent quartz, 2 percent coesite, and 8 percent glass (Kieffer, 1971). Grain sizes in this rock range from 0.1 to 0.2 mm, indicating that it was originally of the massive variety. Quartz grains have been deformed into an intricate network of interlocking pieces resembling a jigsaw puzzle; many grain boundaries no longer have the circular to elliptical shape characteristic of undeformed grains, but contain reentrants and concavities where grains have deformed around each other (Fig. 3a, b). The grains are elongated, and the long axes are aligned to within $\pm 20°$ of the median orientation. The direction of grain elongation was interpreted to be tangential to the direction of the shock front (Kieffer, 1971). Quartz grains show undulatory, patchy extinction when viewed under crossed nicols, indicating the presence of internal strain. Sets of parallel cleavages and fractures pervade nearly every quartz grain. The fractures appear to be closed and may be filled with glass. Planar features (defined as thin planar structures 1–2 μm or less in width and very closely spaced, 2–5 μm apart, which occur in single or multiple sets of five or more [Hörz, 1968, p. 247]) were observed in some grains.

Coesite grains, generally less than 2 μm in diameter, are visible in regions which decorate the edges of original quartz grains. These regions were termed *symplektic regions* by Kieffer (1970, p. 45). The term *symplektic* is used to describe the texture of regions of shocked quartz which, in a thin section of standard thickness, are yellow or gold in transmitted light, and are composed of submicron to micron-sized, high-index crystallites of coesite, areas of glass, and quartz. Quartz generally is visible in optical continuity through the regions. The minerals are intermixed within microns and appear in a vermicular habit; hence, the term symplektic. The texture is illustrated in Figure 3a. The symplektic regions comprise 5 to 10 percent of the area of the thin section. In general

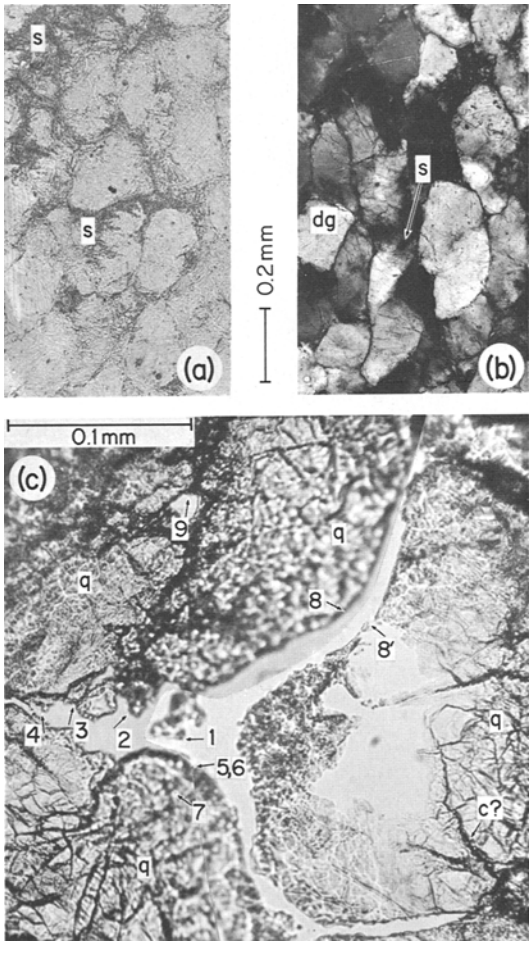

Fig. 3a–c. Optical photographs of Class 2 Coconino Sandstone. **a** Micrograph (plane polarized light) illustrates the deformation of quartz grains and symplektic regions "s" on original grain boundaries. **b** A different region photographed with crossed polarizers, showing deformed grains "dg" and partially isotropic symplektic material, "s". **c** TEM sample after ion thinning. The central area of the figure is unavoidably out of focus due to thickness variations across the ion-thinned sample. The main perforation developed along grain boundaries and extended into the left quartz grain. A small perforation is also visible in quartz at location 9. Veins of symplektic material traverse the quartz grains and rim part of the perforated area. A vein which probably contains coesite is indicated as "c?". TEM observations were made on regions 1 through 8′ and some typical examples are shown in Figure 4–6

the coesite crystals are more abundant near the center of the symplektic region than on the edges. Coesite grains also occur in veins within the quartz grains.

Electron Microscope Observations

A region of the sample which contained abundant symplektic material along quartz-grain boundaries was selected and thinned for observation in the electron

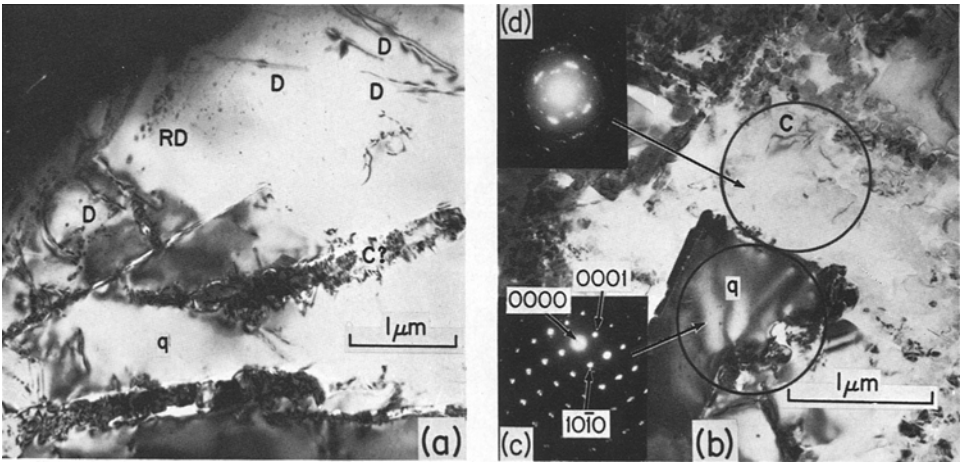

Fig. 4a–d. Electron micrographs of quartz in Class 2 Coconino Sandstone. **a** Quartz in interior of quartz grain; region 8 of Figure 3c. Dislocations "D", radiation damage spots "RD" from the electron beam, and fractures partially filled with a crystalline material which may be coesite "C" are visible. **b** Fractured quartz mixed with coesite and glass near the quartz grain boundary in region 7 of Figure 3c. The diffraction pattern **c** was taken across the large tabular fragment, showing it to be quartz with zone axis [01$\bar{1}$0]parallel to the TEM beam. Tangential spreading indicates approximately 15° misorientation of domains. Asterism of the diffraction spots is probably due to residual internal strain, possibly related to the optically observed patchy extinction in many grains under crossed polarizers. The diffraction pattern **d** was taken on the granular material adjacent to the large grain and shows a strongly misoriented pattern of quartz in orientation similar to (c), and, in addition, weak spots due to intermixed coesite

microscope. During thinning the sample initially perforated along a quartz grain boundary. The perforation spread into a quartz grain, and several lesser holes formed in adjacent quartz grains in different grid-spaces (Fig. 3c). Since this study was particularly concerned with the high pressure phases, an exhaustive study of quartz deformation was not undertaken.

Quartz grains: interior regions. Interior regions of quartz grains (located at some distance from the symplektic material) generally consist of relatively undeformed quartz (Fig. 4a). The dislocation density is relatively low, in the range of $(1 \text{ to } 5) \times 10^8 \text{ cm}^{-2}$. This density is consistent with that observed in grains of sedimentary quartzites (Ardell et al., 1973), and the dislocation substructure is probably that present in the Sandstone in the preshocked condition. Planar features which may be narrow Brazil twins, were observed parallel to (0001) in close association with fractured quartz containing dislocations. Fractures are present in the grains and may be partially open (Fig. 4a). *These observations indicate that the interior regions of quartz in Class 2 rocks have suffered only weak shock damage.*

Quartz grains: boundaries. In regions inferred to be closer to the original grain boundaries, fractured quartz is mixed with coesite and amorphous material (Fig. 4b). Extensive fracture damage and pulverization of the quartz is confined

to a rim of 10 to 100 μm near the grain boundary. In this narrow crushed rim, individual chips of pulverized material have been rotated from their original positions. We suggest that the observed mosaic of interlocked grain shapes in Class 2 rocks has been formed by rotation and shear in such thin outer rims (10 to 100 μm average width), leaving the interiors of grains relatively undamaged. This process produces the appearance of "plastic" deformation noted in thin section by Kieffer (1971), but true plastic flow has not occurred. High dislocation densities ($\geqslant 10^8$ cm^{-2}), which are characteristic of low temperature plastic deformation at relatively rapid strain rates (Ardell et al., 1973), were not observed. Some of the larger (~ 1 μm) fragments of quartz retain their initial low dislocation density ($\sim 5 \times 10^8$ cm^{-2}). The apparent immobility of dislocations in shocked quartz is consistent with static experiments which suggest that extensive plastic deformation is inhibited by high (to 30 kb) confining pressure (Christie et al., 1964).

Along margins of the original grains cracks are present in the form of (1) fractures and (2) grain boundaries between intimately intermixed quartz, coesite and glass in the symplektic material (in all classes of rocks). The cracks are frequently separated by a distance comparable to the wavelength of light. Hence, the partial to total opacity of grain boundary and high pressure phase regions in thin section (Kieffer, 1971) is due to efficient light scattering by the fractures and boundaries between regions of different phases.

Selected area electron diffraction patterns on the fragmented areas at the grain boundaries show strained quartz, coesite (commonly with preferred orientation), and glass to be present in intimate contact (Fig. 4b). The preferred orientation of the small round coesite grains is possible due to the influence of the original quartz grain in controlling the orientation of the nucleated coesite (topotaxy). *Such preferred orientation and the textural relationships at the quartz-coesite constact suggest direct transformation of the quartz to coesite on grain boundaries without an intermediate amorphous or crystalline phase.*

Symplektic material. The central regions of symplektic material are composed of coesite and glass (Fig. 3c, Sites G1, 2, 3, 4, 5, 6, 9). Only the peripheries of the symplektic regions contain intermixed quartz. Coesite occurs in several habits, which are summarized in Table 1.

Regions of coesite are frequently aggregates of particles of unequal size, and differing habits, termed here "Type A" coesite. The material in Figure 5 is dominantly Type A coesite of varying grain sizes, shapes, and textures. Multiple lamellar features parallel to (010) planes are present in most coesite crystals imaged in suitable orientation [with (010) planes parallel to the electron beam]. The features are tens of Angstroms in thickness and give distinct streaking of the diffraction spots in the (010) reciprocal lattice direction (Fig. 5c). These (010) planar structures were also observed in coesite recovered by HF acid extraction. The diffraction contrast from the lamellar features suggests that they are very narrow twins, but the fine scale of the structure (~ 10 Å) prevented us from demonstrating a twin relationship by selected area diffraction. One of us (JMC) has observed optical twinning on (010) composition planes in large synthetic coesite crystals. The presence of submicroscopic twins on (010)

Table 1. Observed characteristics of coesite

Type	Characteristics (TEM/OPTICAL)	Classes Figures	Inferred Origin
A.	Aggregates of small rounded crystals (<1 μm); euhedral or subhedral, frequently twinned. Very little resolvable glass; SAD patterns show preferred orientation	2, 3, 4 Figs. 5, 12, 16	Nuclei or grains of coesite from direct quartz-coesite transition
B.	Coesite-glass mixtures. Fragments of single crystals or clusters of particles in a nonvesicular glassy matrix. SAD patterns range from single crystal (plus glass halo) to polycrystalline (plus glass halo)	2, 3, 4 Figs. 6, 10, 17	Formed by extensive vitrification of Type A coesite
C.	Polycrystalline, polyhedral equidimensional grains in cryptocrystalline cores. Grain boundaries frequently intersect at nearly 120°. May contain twins or stacking faults. Intergrain fractures rare. Very little or no glass	3 only Figs. 13, 14	Nucleated from a hot, amorphous, presumably denser, phase and grew to equilibrium grain shapes

in the space-group assigned to coesite [C2/c in the standard second setting used here or B2/b in the first setting used by Zoltai and Buerger (1959)] raises some interesting questions, as (010) is a mirror plane in the point group (2/m). The twins may belong to (a) a rare category in which the twin operation is a symmetry operation of the point group, but is absent in the space group (there is no mirror plane in C2/c), or (b) they may be related, in view of the pseudohexagonal symmetry around b, by a 120° rotation about b—that is, they may be trillings. However, the presence of twins on the fine scale observed by TEM also suggests the possibility that the crystals on which the structure determination was perfomed may have been twinned on a submicroscopic scale. This would imply that the crystal structure was determined on an "average" twinned structure.

Many coesite grains larger than one micron contain extensive patches of vitreous material intermixed with the crystalline coesite on a scale of tens to hundreds of Angstroms. This is designated "Type B" coesite in Table 1. An example of this is shown in Figure 5a where the circled region appears to be finely polycrystalline, but produced a single crystal diffraction pattern showing a pronounced glass halo. Further examples are shown in Figure 6. In both electron micrographs of Figure 6, domains of crystalline coesite are approximately in single-crystal orientation, as indicated by their diffraction patterns. The coesite domains are generally less than 0.1 μm in length and range in size down to the limit of resolution of the microscope (<50 Å). The larger domains are frequently subrounded in shape. The glass, which appears light grey in electron micrographs, is interspersed among the crystalline material. Since the crystalline domains give single-crystal diffraction patterns, we infer that large

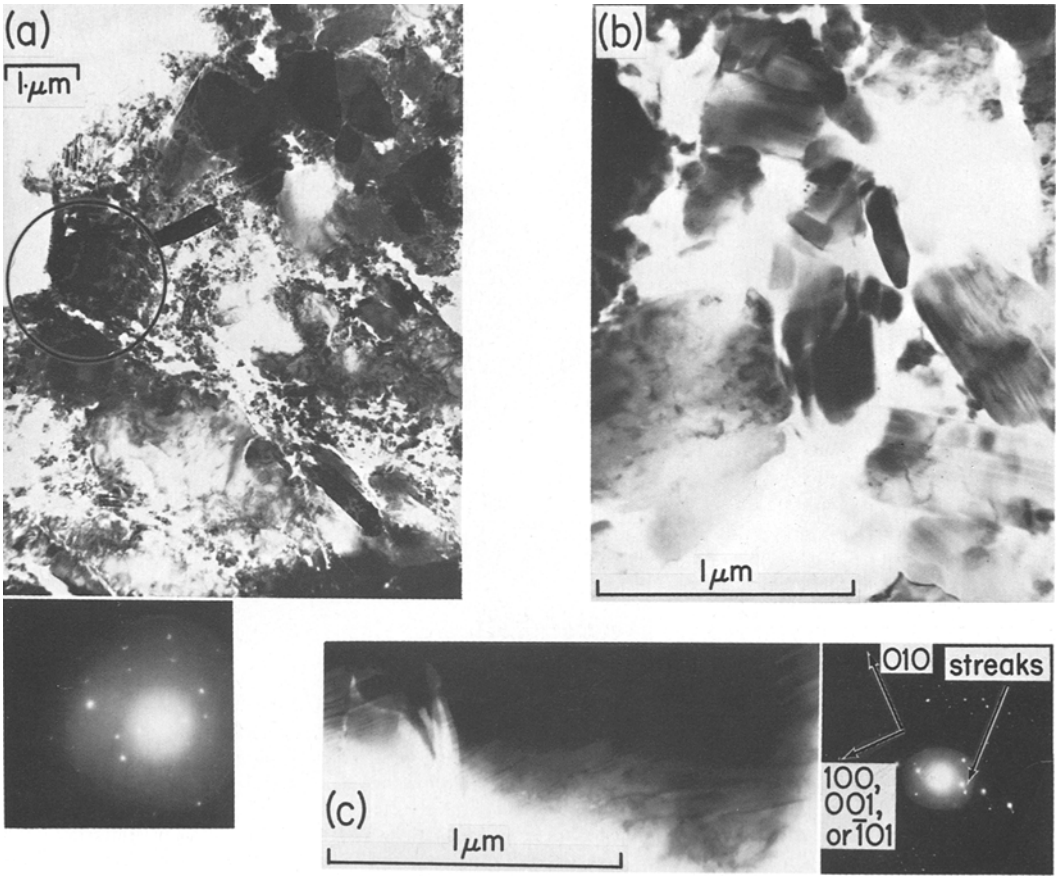

Fig. 5a–c. Electron micrographs of coesite in Class 2 Coconino Sandstone. **a** Region 6 in Figure 3c. Bright field micrograph of a complex region of coesite of widely varing grain size. The associated diffraction pattern was taken on the fine grained material in the encircled region. All spots appear to be from a single crystal of coesite with zone axis [$\bar{1}$01] parallel to the electron beam; the diffuse halo is due to intermixed glass. **b** Tabular twinned crystals of Type A coesite from region 1 in Figure 3c are shown on the right side of this micrograph. The largest grain at the lower left has fragments of coesite remaining in a generally glassy matrix, a texture typical of Type B coesite. Figure 6 shows more examples of this texture. **c** This coesite grain from region 3 of Figure 3c has twins or stacking faults at a scale of tens of Angstroms. These features are parallel to the trace of (010) and cause the streaking indicated in the diffraction pattern. The pseudohexagonal symmetry of the monoclinic coesite lattice allows several assignments for the zone axis: [00$\bar{1}$], [100], or [101].

single crystals of coesite initially formed in these regions and subsequently partially inverted to glass of thetomorphic character. No evidence of a molten state is present in the form of vesicles or schlieren. We cannot rule out the possibility of intrusion of the glass into pre-existing cracks from a nearby source, but do not consider this likely. These are the first reported observations of thetomorphic glass in a high pressure phase and demonstrate that the thetomorphic glass is produced late in the shock event, after sufficient time has lapsed to allow the growth of relatively large coesite grains.

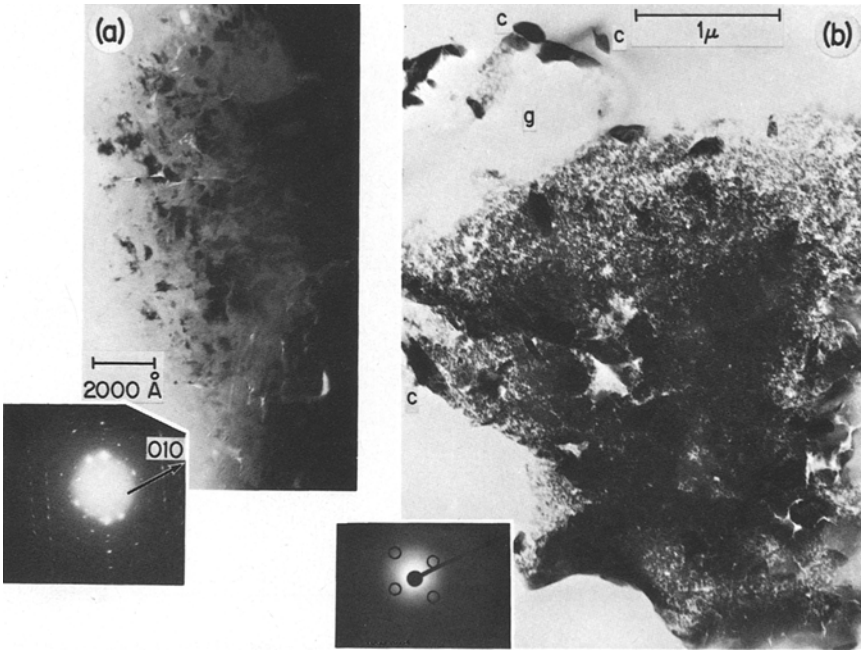

Fig. 6a and b. Electron micrographs of coesite and thetomorphic coesite glass in Class 2 Coconino Sandstone. **a** Region 5 in Figure 3c. The bright field micrograph shows domains of coesite (dark areas) interspersed in glass (light grey areas lacking diffraction contrast). The selected area diffraction pattern was purposely overexposed to show the streaking of diffraction spots; glass halo can be seen on the original negative. The diffraction pattern shows a single crystal pattern of Type B coesite. **b** Region 9 in Figure 3c. Small round domains of coesite (dark, strongly diffracting areas labeled "c") of nearly uniform orientation are embedded in glass (light grey material of uniform contrast labeled "g"). The associated diffraction pattern was taken from an area enclosing domains "c" at the top of the micrograph. The glass halo is very strong, but about a dozen very faint spots are visible in the diffraction pattern, which is basically a single crystal pattern. Four of the spots are circled. Lower right part of the figure shows clusters of fragmentary remains of a large grain

Small rounded domains of coesite are generally seen in remnant, partially vitrified single crystals (Fig. 6b). These rounded grains may occur as individuals in the glass (Fig. 6b, upper left) or in clusters in the partially vitrified coesite (Fig. 6b, lower right). From the example in Figure 6, we infer that ellipsoidal or subspherical grains (such as in Figure 6b, lower left) may be fragmentary remains of larger grains which have partially inverted to a vitreous, or partially vitreous, state.

Type B coesite resembles Type A coesite in grain size and texture, e.g., evidence of twinning may be found in some Type B grains, and it occurs in similar locations in the rocks. We infer that Type B crystals are partially vitrified remnants of Type A crystals (Table 2).

In summary, in Class 2 rocks a direct transition from quartz to coesite takes place in a zone of 10 to 100 μm width along original quartz grain boundaries in the zone of extensive crushing of quartz. Single crystals of coesite up to 5 μm in length were formed initially, but some (in fact most of those

observed) have subsequently inverted partially or totally to glass. Small domains of crystalline material are preserved within the glass. Glass is present in three forms: (1) as lamellae in the quartz, where it is unassociated with coesite and must have originated directly from the quartz; (2) as networks in partially inverted coesite grains, where it clearly was derived from the coesite itself; and, in a very few places (3) as microvesicular lechatelierite. The presence of lechatelierite in Class 2 rocks is not expected from equation of state properties and must be attributed to great pressure and temperature inhomogeneities during the shock.

5. Class 3 Rocks

Petrographic Description

The characteristic Class 3 sample (No.33, Fig. 2) selected for this study was a dense white rock. The rock ($10 \times 8 \times 2$ cm) was found in alluvium formed from mixed debris and stratified debris on the crater rim on the southeast side of the crater. The exterior surface was stained light brown from weathering. A weakly developed parallel platy structure, accentuated by weathering, was visible on the original surface of the rock and on freshly broken surfaces. The parallel segments were approximately 5 mm in thickness and the plates were separated by less than 0.05 mm. Individual grains were not resolvable in hand specimen.

By X-Ray diffraction the composition of the rock, after removal of calcite, which constituted approximately 2.5 weight percent of the rock, was determined to be 72 percent quartz, 21 percent coesite, $\leqq 1$ percent stishovite, and 7 percent glass (Fig. 1 b).

The original quartz grains have been deformed by passage of the shock wave. The grains are elongate and aligned (Kieffer, 1971, Fig. 8), presumably parallel to the plane of the shock front. The size distribution of the grains is unimodal (area ~ 0.04 mm^2) and we conclude that this was originally a massive rock.

Quartz grains in this Class 3 rock resemble quartz grains in Class 2 rocks. They contain abundant cleavages, irregular closed fractures (some of which may be healed with glass), occasional step-faults, and planar features. Small isotropic areas are observed on some grain boundaries. A few percent of the quartz grains contain crystals of a few microns diameter. These grains have a high index of refraction and are believed to be coesite. Coesite crystals are also found locally along fractures through a whole grain or in parallel cleavages. A few quartz grains (< 2 percent) are completely fragmented into 100 μm pieces and are intermixed with coesite crystals.

In thin section nearly every quartz grain is bordered by symplektic or opaque material. The opaque material is a mixture of coesite, glass and stishovite, as shown by X-ray diffraction of selected areas (Kieffer, 1970, 1971). Eighty to ninety percent of the symplektic and opaque material is located on quartz-grain boundaries. The boundary between opaque material and quartz may be sharp (~ 2 μm) or grade through 10 to 20 μm of symplektic material.

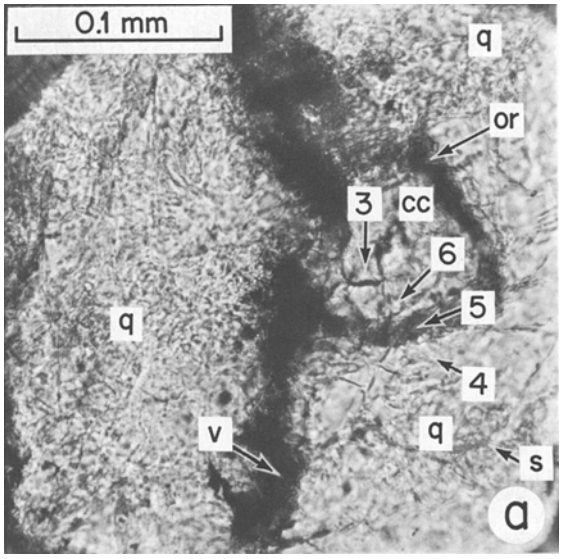

Fig. 7a and b. Optical photographs of a typical region examined in Class 3 Coconino Sandstone, sample 33. **a** Region containing quartz "q" and high pressure phases: an opaque vein "v", symplektic material "s" near the vein and within the quartz grain, an opaque rim "or" surrounding a core of cryptocrystalline coesite "cc". **b** The same region after ion thinning. The quartz thinned much more rapidly than regions containing coesite; consequently the vein and opaque rim are left unsupported by the removal of quartz. TEM observations were made in the relatively undamaged regions of quartz, "4", more extensively damaged quartz near the boundaries of the original grains, "5", the opaque rim "6", and the core of cryptocrystalline coesite, "3". Many other regions were examined in a similar manner

Thirty to fifty percent of the opaque regions contain a clear, single or double core of high index material in their center (Fig. 7). Henceforth in this paper the word "core" refers specifically to these regions or their analogues composed of vesicular glass in Class 4 rocks. The cores were identified as cryptocrystalline coesite on the basis of their index of refraction and the appearance of lines characteristic of coesite in X-ray diffraction patterns. The boundary between opaque material and the cryptocrystalline coesite cores is usually sharp ($< 10\,\mu m$). Typically the cores measure 60 to 100 μm in longest dimension, but they may be as long as 200 μm. Small crystallites of microcrystalline coesite penetrate the outer regions of the cores, and small opaque veins may crisscross the cores. The cores nearly always display a network of clear fractures or veins that subdivide them into small round or oblate "cells", which are generally less than 30 μm in diameter (Fig. 7). The texture of the core resembles a mud-cracked surface. In a thin section of standard thickness, most of the cores are isotropic with only a few 10 μm areas showing weak birefringence. In an ultra-thin section (such as a thin edge of the standard thin section), it is possible to see that the individual "cells" or groups of two or three "cells" display weak and patchy birefringence. We consider that these may be single coesite crystals. The absence of birefringence in thicker areas of the section is probably due to overlap of several crystals.

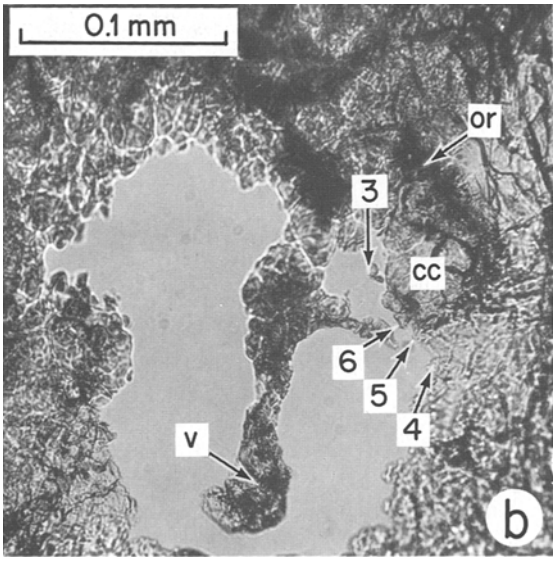

Fig. 7b

Areas Selected for Electron Microscope Observations

Several discs were ultrasonically cored from a doubly polished thin section for thinning and examination by transmission electron microscopy. In particular, the cryptocrystalline cores and surrounding symplektic regions containing high-pressure phases were well represented in these areas. Four discs were examined in the electron microscope, some after repeated rethinning by ion bombardment and observation in the microscope. A photograph of a typical region is shown in Figure 7. As each specimen thinned, initial perforations tended to form in quartz regions. We then carefully allowed the perforations to grow until the opaque material and cryptocrystalline core had been breached. Observations with the TEM were then made along the hole boundary in quartz, opaque, and core material. A total of eight high-pressure regions and adjacent material were observed. Electron micrographs and diffraction patterns were obtained in six of these.

Electron Microscope Observations

In the following section we attempt to describe our observations without interpretation of the conditions of origin of the features, except where this is obviously indicated. However, in order to organize the data from over three hundred photomicrographs, diffraction patterns, and visual observations, we have treated the observations according to the sequence: (1) quartz, (2) symplektic and opaque regions, and (3) cryptocrystalline core material. To the extent that the original model (Kieffer, 1970, 1971) of high pressure phase formation is correct, this order of phase assemblages represents a sequence of increasing pressure and temperature conditions.

Quartz. Regions of relatively undeformed quartz with diameters as large as tens of microns are observed in grain interiors. In these interior regions dislocations are generally preserved (Fig. 8a). We estimate that up to 50 percent of the residual quartz in the Class 3 rocks may be in such an undeformed state.

The remaining quartz is fragmented by numerous sets of subparallel partings, usually along crystallographic planes (Fig. 8b, c), and irregular fractures (Fig. 8a, b). Some of the parallel partings are slightly curved, and the quartz slices locally show marked strain. Generalized strain contrast is evident in the quartz slices, suggesting that many of the fractures are healed, a conclusion supported by the fact that the quartz has retained its cohesion through the ion-thinning and handling process. Although many partings or planar features are completely filled with glass, some are partially or wholly open (Fig. 8c). Some of the open fractures are partially filled with "froth" (Fig. 9). We discuss the properties and origin of this froth in later sections. Partings in the quartz grains occur on a scale down to at least 15 Å. Irregular fractures are observed to traverse the finer parallel partings.

Closely spaced regular planar features parallel to the basal plane showing fringe contrast and in some cases apparently containing dislocations, were observed in a few regions of the quartz, notably near grain boundaries and in proximity to the coesite (Figs. 8d and 12). Similar features have been observed in natural quartz crystals deformed at relatively low temperature ($\sim 500°C$) and "rapid" strain rates ($\sim 10^{-4}$ to 10^{-5} s^{-1}; McLaren et al., 1967) and were interpreted as Brazil twins parallel to the basal plane. Similar features have also been observed by the authors (Phakey and Christie, unpublished data) associated with the basal deformation lamellae in shatter cones in the Jeppestown Sandstone from the Vredefort structure in South Africa (Carter, 1965). The Jeppestown sandstone contains many shatter cones and is considered to have undergone shock deformation. These features, which we tentatively call "Brazil twins", were observed in Class 2 and 3 rocks and probably occur in the appropriate regions of Class 4 rocks, although they were not observed due to our limited observations on the crystalline quartz. In the instances where the "Brazil twins" were observed, they are in close proximity to coesite grains, indicating stresses over 30 kb and probably in the range of 30 to 130 kb.

Symplektic and opaque regions. The symplektic and opaque regions contain intimate mixtures of phases, with grains generally too small to be identified optically. TEM observations showed that the phases present include quartz, coesite, stishovite and cryptovesicular material that we have referred to as "froth".

Coesite generally occurs as granular-looking aggregates with uneven contrast, up to several microns in size, in direct contact with quartz (Fig. 10a) or locally separated from quartz by narrow zones or lenses of froth (Fig. 10b, c). The inference from the common quartz-coesite contacts is that in many places the transformation to coesite proceeded directly from quartz. The regions of coesite with granular appearance are deceptive, as their diffraction patterns commonly show that the grains have a very limited range of orientations (Fig. 10a) or are, in fact, single-crystals (Fig. 10b).

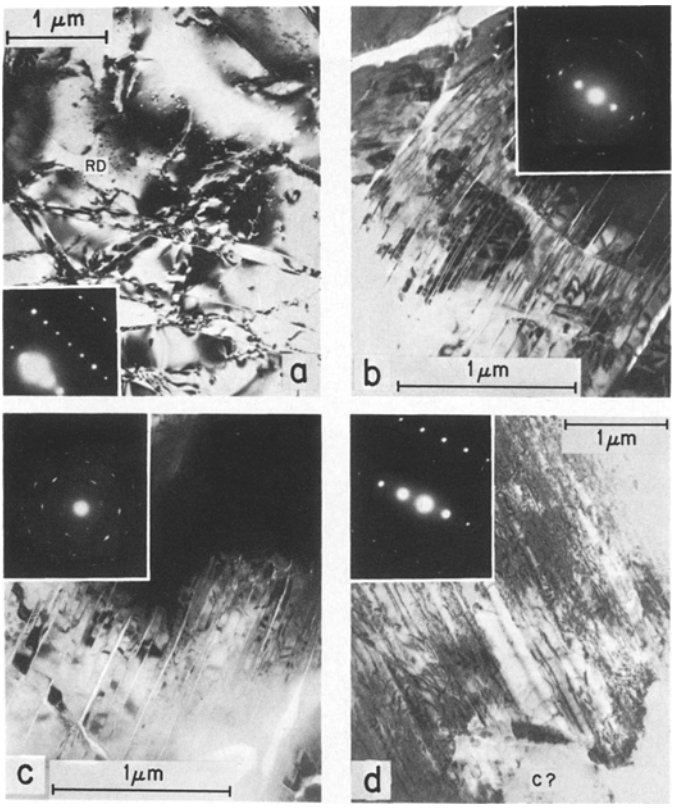

Fig. 8a–d. Electron micrographs of weakly damaged quartz in Class 3 Coconino Sandstone. **a** Fractured quartz. Dislocations are visible in the quartz between the fractures. Radiation damage "RD" from the electron beam is visible as a "measle"-like spotting. The fractures are closed. **b, c, d** Electron micrographs of planar features in quartz in Class 3 Coconino Sandstone, region 4 in Figure 3c. **b** Glass filled cleavages along $(10\bar{1}1)$ planes in quartz. Streaking of the central spot on the diffraction pattern indicates "boundaries" present on a scale as fine as 15 Å. We believe that these boundaries may be the edges of small lens-shaped cavities of glass. Note the rather large rotation of several fragments on the left side of the micrograph, causing asterism in the diffraction pattern. **c** Open cleavages and cross-cutting irregular fractures in quartz. **d** Planar features on (0001) in quartz. These features were commonly observed in regions near the high pressure phases (see, e.g., similar features in Fig. 12). Here they are in contact with a region, labeled "c?", whose texture resembles that of partially vitrified coesite (compare with the lower left grain in Fig. 5b)

Stishovite was identified definitely by means of diffraction patterns in two regions (Figs. 11 and 12). In both cases it occurs in direct contact with quartz and, in one case (Fig. 12), also in contact with coesite. The nature of the coesite-stishovite contact cannot be established from the contact in Figure 12, but in Figure 11, the contact between the quartz crystal and finely polycrystalline stishovite ($\sim$500 Å) is characterized by an intimate mixture of the two phases and is interpreted as indicating a direct transition from quartz to stishovite. There is no evidence to suggest that an intermediate glassy or crystalline phase was formed. The completely polycrystalline nature of the stishovite diffraction

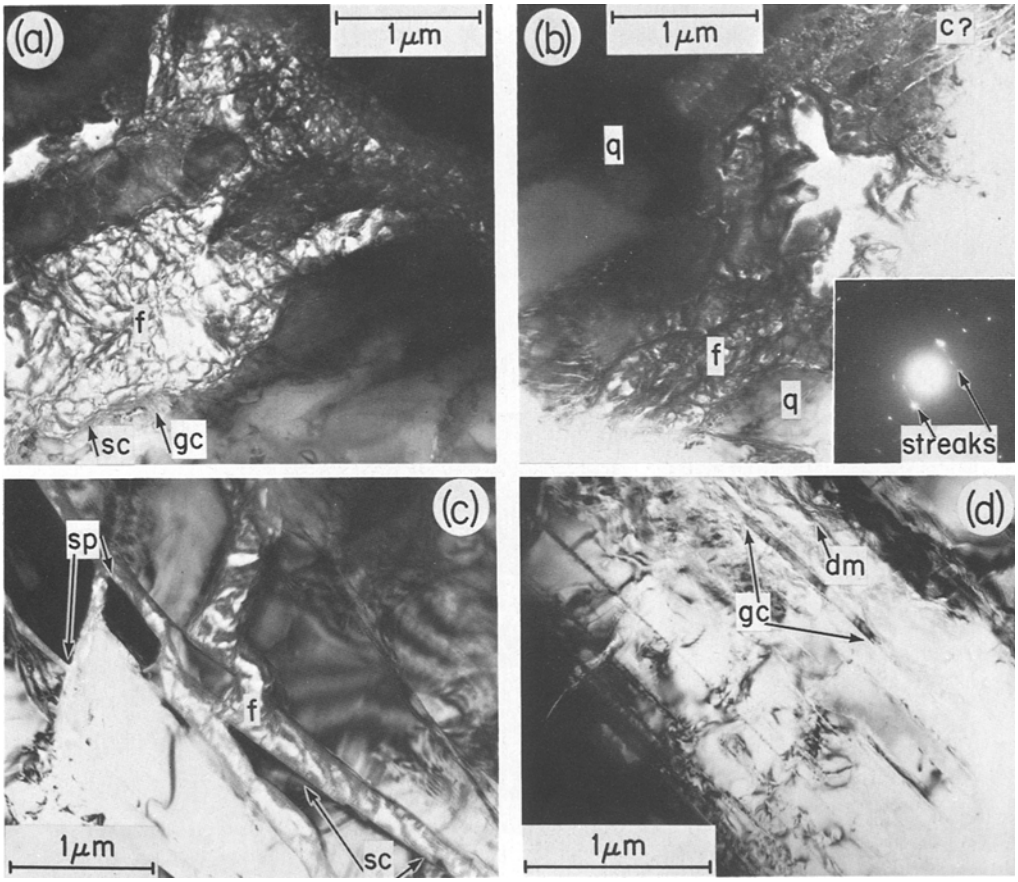

Fig. 9a–d. Electron micrographs of froth in Class 3 Coconino Sandstone. **a** Froth " in an irregular hole in quartz, showing both sharp contacts "sc" and gradational contacts "gc" with crystalline quartz; **b** Froth in quartz very near the region containing stishovite, shown in Figure 12; coesite "c?" is probably present in the upper right corner. Streaks in the diffraction pattern are apparently caused by the small, poorly resolved planar features in the upper right corner. **c** Froth in fractures in quartz showing sharp contacts "sc" and sharp points "sp" on fragments of quartz surrounded by froth. Both of these relationships are interpreted to indicate that, in this location, the froth did not react appreciably with quartz during its formation or deposition. **d** Froth in regular, partially healed fractures in quartz in a symplektic region. In a few places the froth contains dark material "dm" which diffracts electrons and therefore must be finely crystalline. The gradational contacts "gc" with quartz slices visible in this micrograph are interpreted as evidence that the froth reacted with, or formed from, quartz in this region

Fig. 10a–e. Electron micrographs of coesite in symplektic and opaque material in Class 3 Coconino Sandstone. **a** A 2 μm grain of partially vitrified coesite "c" is embedded in the boundary region of quartz "q". Submicron crystalline fragments (arrow "cf") of quartz are bounded by narrow fractures. The patchy contrast in the coesite grain is caused by misorientations of small domains through a few minutes of solid angle. This causes the tangential spread of single crystal coesite spots on the diffraction pattern **b** A 4 μm grain of coesite "c" containing vesicular froth "f" embedded in a single crystal of quartz "q" which shows cleavages of identical orientation in both the right and left segments. In serveral places the coesite grain is in direct contract with the quartz grain, but in many other places the coesite is separated from quartz by a 0.01 to 0.20 μm band of

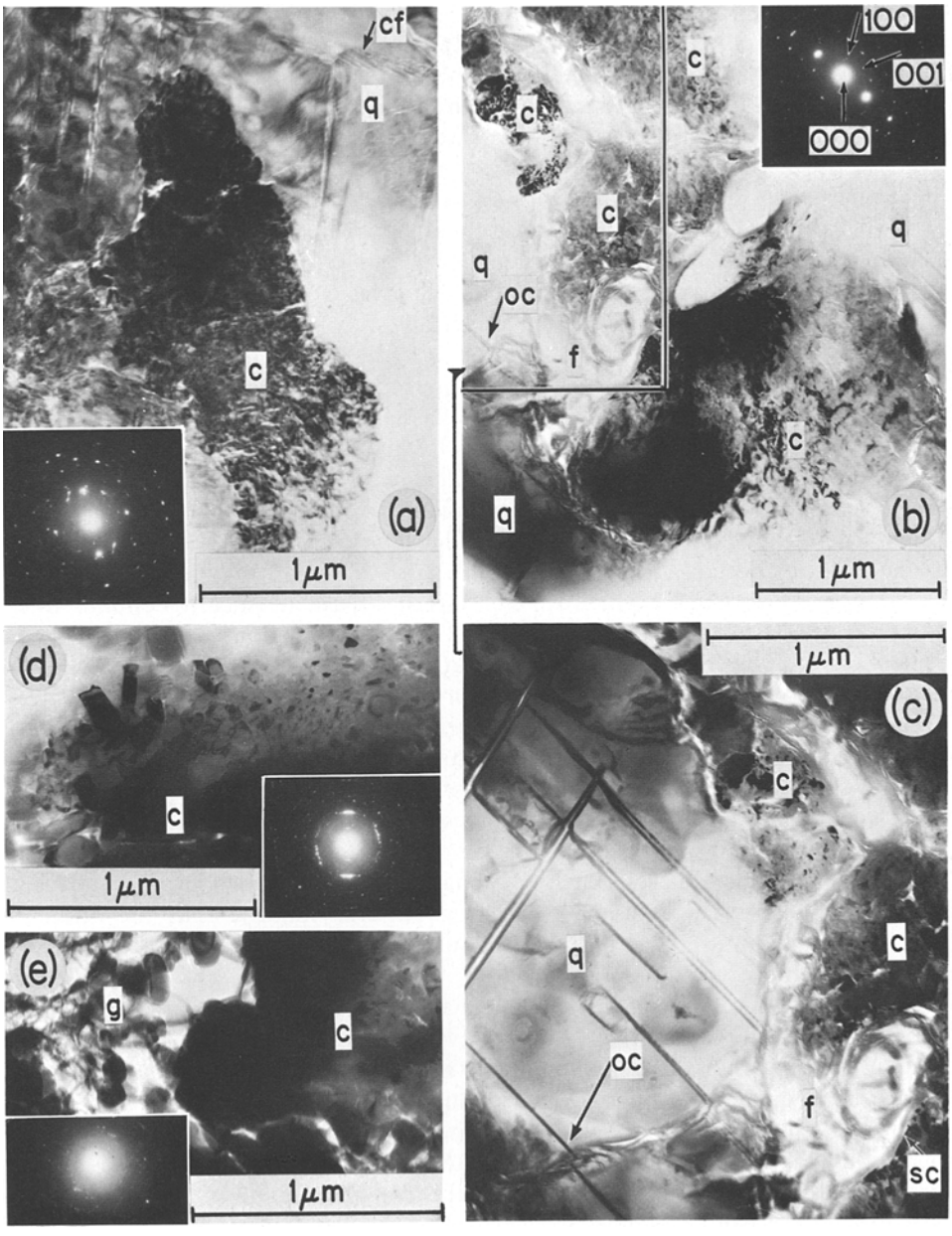

froth [see enlargement (c) below]. The froth is amorphous in most places, but is diffracting and therefore crystalline in other places. The froth alters cleavage traces [arrow "oc" in (b) and (c)]. **c** Enlargement of the quartz-coesite contact in (b). A sharp contact "sc" visible between the coesite and froth in the lower right corner is gradational in other parts of the grain. **d** and **e**. Partial vitrified coesite in region 5, Figure 7a, b; the sites are within a few microns of each other. In **d** the coesite retains the thetomorphic texture and traces of single-crystal orientation in the diffraction pattern; in **e** it is nearly polycrystalline and is mixed with vesiculated glass, a rare feature in the Class 2 rocks. Both diffraction patterns show a glass halo and index as coesite

pattern indicates that the grains are randomly oriented, probably as the result of massive reorientation of bonds involved in the change from four-fold to six-fold coordination. The presence of froth in narrow zones between stishovite crystals and in thin fissures traversing both the quartz and stishovite in Figure 11 indicates that the froth originated after the quartz-stishovite transition.

The stishovite grains in Figure 11 are nearly equidimensional; they do not resemble those in chemically separated samples which we studied. The grains shown in Figure 11 are probably too small to be recovered by the standard HF-acid technique. The grains in Figure 12, however, range up to several thousand Angstroms in diameter and are in some cases elongate, so that they might correspond to the material in our chemically recovered sample and to that described by Holm et al. (1967).

Quartz, coesite, and stishovite are intermixed within small areas only a few microns across, as is seen in Figure 12. It is clear from the phase diagram of SiO_2 (Fig. 2a) that no equilibrium P-T-V conditions exist where all three phases are simultaneously stable. The coexistance of these phases across regions of less than a thousand Angstroms in diameter indicates great variations of pressure and temperature locally within the shock, or nonequilibrium reaction conditions, or both.

Amorphous material which we call "froth" characteristically contains fine angular vesicles. It always occurs in proximity to or within the high pressure phase region. The characteristic relations are illustrated in Figure 9, which shows relations between froth and quartz; Figure 14, which shows froth and coesite; Figure 11, which shows froth at the quartz-stishovite contact; and, Figure 13 which shows froth in a coesite core. Froth constitutes a relatively small proportion of the symplektic aggregate (perhaps 20 to 40 percent by areal extent and much less by weight percent). It occupies veins and fractures near the edges of the quartz grains and occurs as narrow selvages along grain boundaries in all of the other phases. Lack of image contrast on micrographs and the presence of glass halos in the diffraction patterns indicate that the cellular walls of the froth are generally amorphous. In a few places e.g., in Figure 9d, the froth contains crystalline material.

The textural relationships between quartz and froth are illustrated in Figure 9. The froth occurs in veins up to several microns wide, in irregular open fractures traversing quartz grains, or in thin planar fissures in grains. In some cases the boundary between the quartz and froth is sharp, as if the froth had been injected into an open fracture, and in others the boundary is gradational, as if there had been reaction between the froth and the quartz wall or as if the froth had been developed from the neighboring quartz. The amount of silica in the froth is small. Typical frothy zones are probably considerably more than 50 percent porosity. In places (Fig. 9c) very sharp corners remain on the host quartz grains, suggesting that these fragments were unaltered by the froth.

The froth can easily be distinguished from lechatelierite, which contains much coarser, more nearly spherical vesicles (and is found mainly in Class 4 rocks), and from the homogeneous, bubble-free, thetomorphic glass that replaces the quartz and coesite. Since the characteristic vesicular structure of the froth could not exist under high pressures, we infer that it was formed at a late

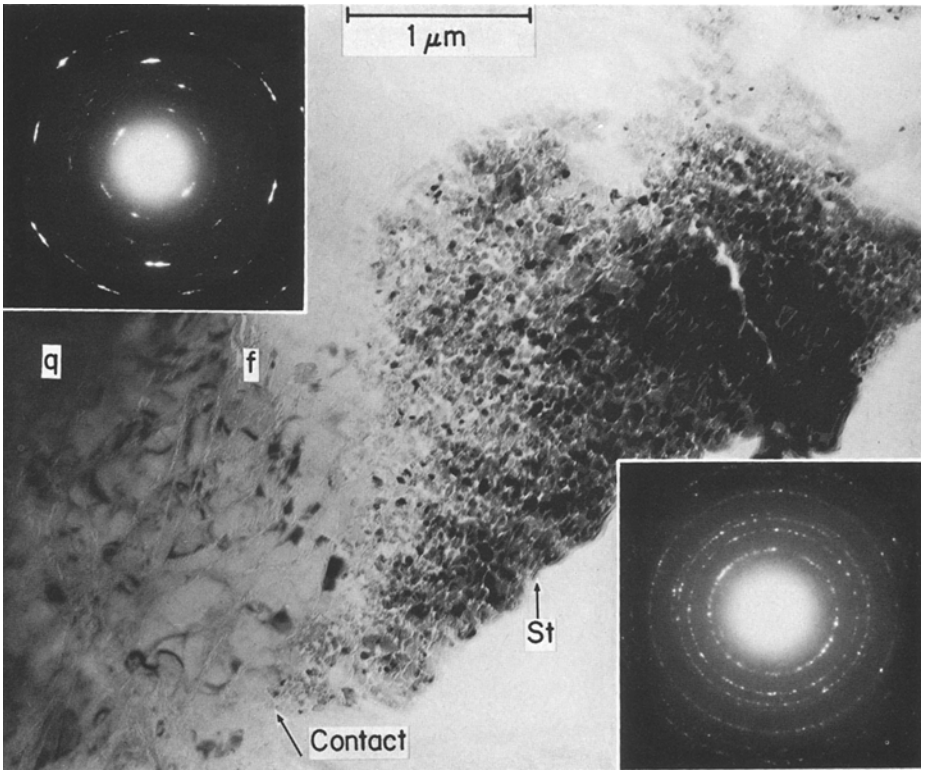

Fig. 11. Electron micrograph of quartz-stishovite contact in Class 3 Coconino Sandstone. Quartz, "q", is in direct contact with stishovite, "s". The transition region within the quartz is fractured subparallel to the contact between the two phases, "contact", and the fractures contain froth "f". Top left hand diffraction pattern is of quartz and shows misorientations in the quartz up to approximately 10°. Bottom right diffraction pattern shows a polycrystalline pattern for stishovite; individual grains of stishovite are less than 500 Å in diameter. Stishovite and quartz appear intermixed only in a thin region of less than 1,000 Å width

stage in the rarefaction event. One of the characteristic occurrences of the froth is in thin concentric fissures between quartz and fine-grained coesite and stishovite (Figs. 11 and 12); these fissures may have formed as pull-away features between the dense phases and quartz during the rarefaction or may have been the sites of water during the shock (discussed in further detail in Section 9).

The opacity of the "opaque regions" appears to be associated mainly with submicroscopic veins of the froth near the boundaries of quartz grains and in the high-pressure phase regions. Because many of these veins are superposed in a standard optical (30 μm) section, the opaque regions appear quite wide. As the standard sections underwent ion thinning, the opaque regions became smaller and eventually were resolved into thinner zones or groups of veins (Fig. 7). The networks of froth (with 10–500 Å vesicles) are most probably the major cause of scattering that gives rise to the opacity in Class 3 rocks. Additional scattering can be caused by any coarsely vesicular lechatelierte present and by optical discontinuities associated with submicroscopic coesite and stishovite grains.

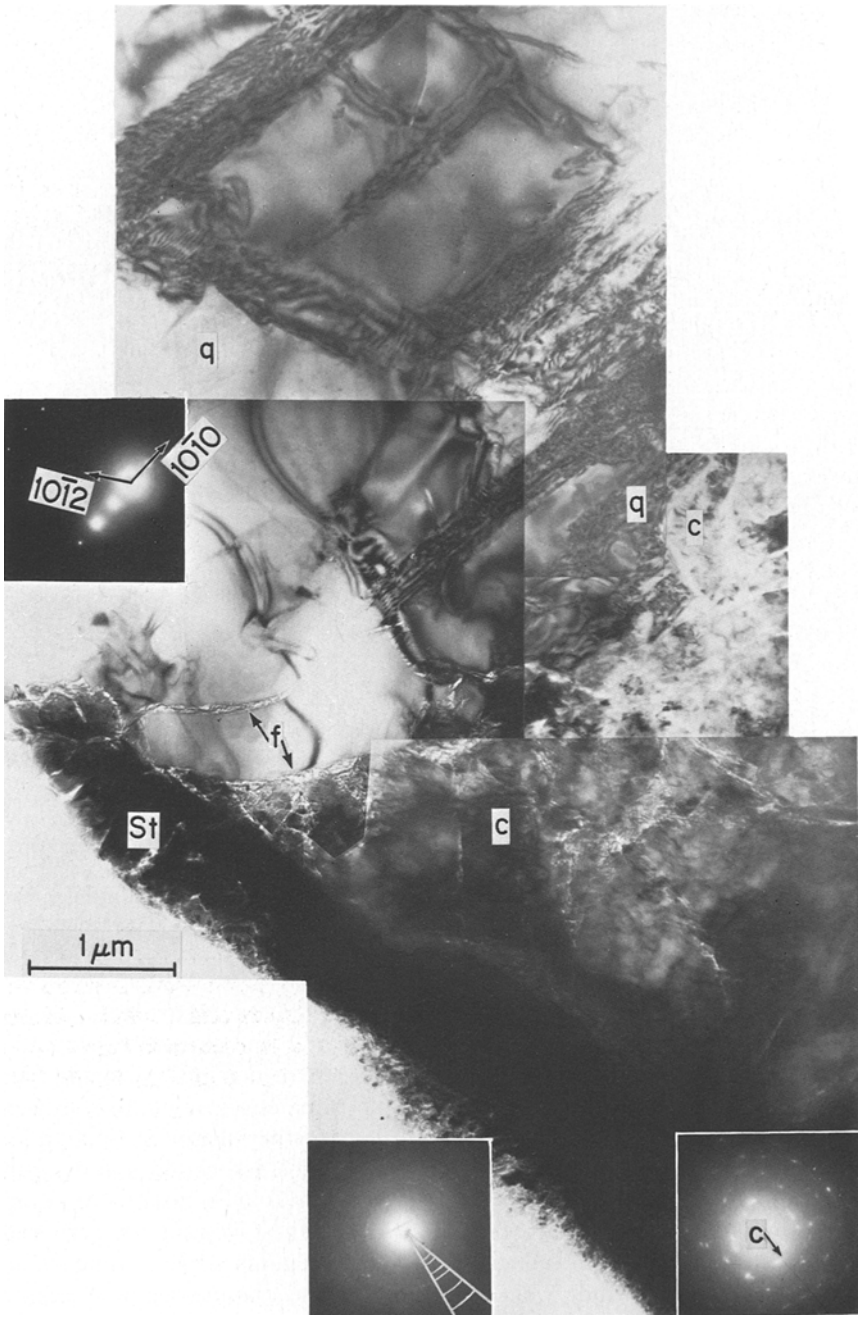
q
$10\bar{1}2$
$10\bar{1}0$
q
c
f_1
St
c
1 μm
c

Cores. The cryptocrystalline cores are composed predominantly of an equigranular mosaic of coesite (Figs. 13 and 14). We have called this "Type C" coesite in Table 1. Numerous electron diffraction patterns of single crystals and polycrystalline groups of this material were indexed.

In general the coesite grains are polygonal, equant or slightly elongated, and of very uniform size (1 ± 0.5 μm), Figure 13. The core grains are therefore generally smaller than the deformed and partially vitrified coesite crystals in contact with quartz in the symplektic regions.

Coesite grains in the core commonly show very fine and closely spaced (~ 15 Å to 400 Å) planar features on (010). The diffraction contrast from these planar features suggests that they are twins and not stacking faults.

Triple junctions of grain boundaries commonly subtend angles close to 120°, indicating an "equilibrated" texture (Fig. 14). This unique texture within the shocked rocks implies a history of pressure and temperature quite different from the coesite formed elsewhere in the rocks. Such a texture is common in annealed or recrystallized metals and single-phase mineral aggregates and is referred to by metallurgists as a "mature" polycrystalline structure (Smith, 1964). The interfaces formed by impingement of similar grains have adjusted their positions according to internal properties of the material to form a foam structure. In such structures the effects of the history of nucleation, growth, and impingement on grain shape are largely obliterated, although the number of surfaces shared with neighboring grains is related to this history. To form equilibrium dihedral angles of 120°, the surface (grain-boundary) tensions in all three boundaries must be equal. The frequent occurrence of angles close to 120° in the two-dimensional sections of coesite therefore suggests little anisotropy of the surface or grain-boundary energy in coesite.

The grain-shape varies somewhat from one core to another. In some cores (Fig. 14a) the grains are angular, with tight boundaries; froth-lined interstices up to several hundred Angstroms thick are present along only a few grain boundaries in this core (Fig. 14b). In contrast, in the core illustrated in Figure 13, the grains have rounded corners, although the equidimensional and polygonal character of the grains is still preserved; the grain boundaries are all occupied by zones of froth up to 1,000 Å wide. The vestiges of the equilibrated texture suggest that this aggregate was originally similar to that in Figure 14a and that the grain margins were corroded and replaced by froth, apparently very late in the rarefaction part of the shock event. In a few regions near the margins of the coesite cores, the structures were observed to be so complex and to contain so much froth that the core texture was barely recognizable and identification of the core material relied solely on the diffraction pattern. Kieffer (1970, 1971) reported an average index of refraction of four cores extracted

Fig. 12. A composite electron micrograph showing nonequilibrium phase relations in Class 3 Coconino Sandstone. The quartz "q" shows planar features which may be Brazil twins. The coesite "c" is polycrystalline, as is the fine-grained stishovite "St". At the intersection of the three phases, froth "f", which is characteristically present in the high-pressure phase regions in Class 3 rocks, is visible. Diffraction patterns on the three phases were centered on the sites labeled "St", the left "q" and the bottom "c". These diffraction patterns clearly show the presence of three distinct phases mutually in contact

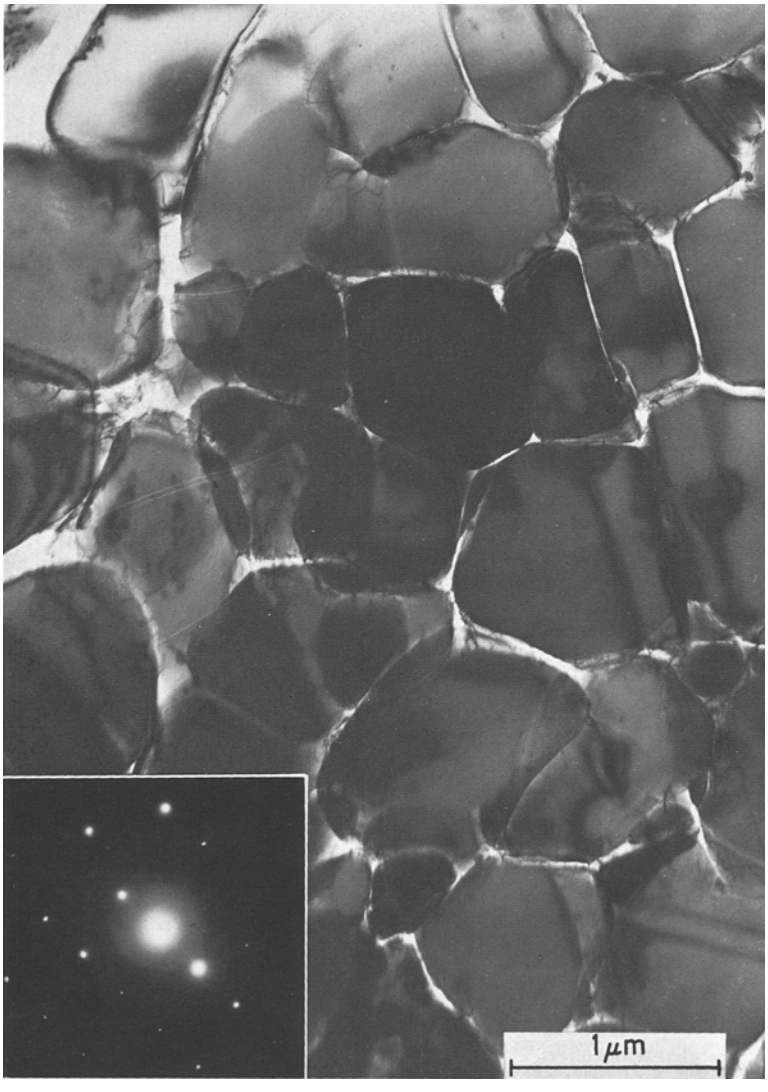

Fig. 13. Electron micrograph of cryptocrystalline coesite core material in Class 3 Coconino Sandstone, site 3 in Figure 7a, b. This micrograph illustrates the equidimensional grain size and mosaic texture characteristic of core material, although the froth present at nearly all grain boundaries has eroded the originally tight contacts (compare with Fig. 14a). Twins or stacking faults are present in some grains. The diffraction pattern is from a single grain in this group, and shows single crystal coesite

from crushed grains as 1.584 ± 0.004, slightly lower than the reported indices of coesite ($\alpha = 1.599$, $\gamma = 1.604$ [Coes, 1953]). This lower index may now be attributed to the occurrence of submicroscopic intergranular froth in the cores (Fig. 13).

In summary, many of the features observed in Class 2 rocks also occur in Class 3 rocks: regions of relatively undeformed quartz, highly fractured quartz

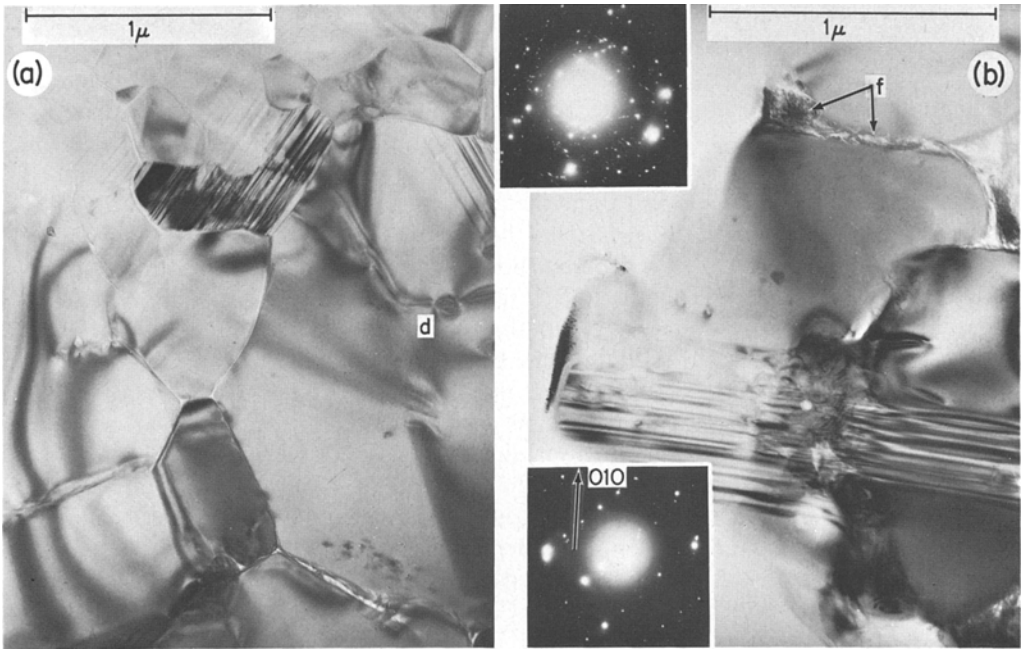

Fig. 14a and b. Electron micrographs of cryptocrystalline coesite core material in Class 3 Coconino Sandstone. **a** This cryptocrystalline coesite shows the characteristic mosaic texture with unimodal grain size, 90° and 120° dihedral angles, twins or stacking faults, dislocations, and a slight bit of froth between the grain boundaries at the bottom of the micrograph. Grains in upper left corner show preferred orientation. The diffraction pattern shows polycrystalline coesite with streaking of spots normal to the predominant twin direction in the upper part of the electron micrograph. **b** These grains from coesite core material show well developed twins on (010). The diffraction pattern is off zone axis, and five Laue zones are present. Moiré interference patterns are present in the center of the field of view. Notice the froth "f" between the grain boundaries

on grain boundaries, symplektic material and thetomorphic glass. In addition, stishovite, froth and cryptocrystalline core coesite are characteristic of Class 3 rocks.

6. Class 4 Rocks

Petrographic Description

The Class 4 sample selected for this study was a dense, white hand specimen measuring $10 \times 8 \times 6$ cm. It was collected on the south terrace of Meteor Crater. The surface of this rock was stained light brown from weathering. Parallel, discontinuous, sinuous tension fractures which are a few tenths of a millimeter to millimeters in width and up to several centimeters in length, traverse the rock. These features were described as typical of glass-bearing Coconino Sandstone by Chao (1967, p. 206). The fractures are commonly lined with calcite (5 percent of the rock by weight). X-ray diffraction analysis of the

rock after removal of calcite yielded a composition of 40 percent quartz, 17 percent coesite, and 43 percent glass (Fig. 1b).

In thin section the quartz grains appear to be isolated in a matrix of opaque material and vesicular glass (see Kieffer, 1971, Fig. 11). Nearly every quartz grain is rimmed with a thin symplektic region and a border of opaque material (Fig. 15). Coesite and glass occur in symplektic and opaque regions on quartz grain boundaries, in veins pervading the quartz grains, in opaque material lining cleavages, and in small regions scattered throughout the quartz grains. The opaque material frequently forms a continuous border up to 100 microns in width around 10 to 20 quartz grains (Kieffer, 1971, Fig. 11). Figure 15 shows a small opaque rim. Vesicular "cores" occur within the opaque rims. The cores are largely amorphous, but generally contain some birefringent fragments.

Quartz grains are heavily fractured and show planar features and cleavages. Up to 75 percent of the residual grains may be similar to the original grains in size, but a substantial number of smaller quartz fragments are visible in thin section. They appear to have been heavily damaged and partially converted to high-pressure phases, glass, and possibly to recrystallized quartz (Rogers, 1929), although we did not definitely identify the latter.

Optically resolvable regions of melted silica glass, lechatelierite, in the Coconino Sandstone occur principally in the Class 4 and 5 rocks. The glass in Class 4 rocks occurs in cores which measure up to several millimetrs in diameter (Fig. 15). The glass contains innumerable spheroidal vesicles which range up to several tenths of a millimeter in diameter. Most vesicles, however, are less than 10 microns in diameter and occur so profusely in parts of the glass cores as to cause opacity. Variation in vesicle abundance causes variation in light transmission porperties. Schlieren and elongated vesicles in some cores indicate shear within the molten glass.

The region studied (Fig. 15) in the electron microscope contained a roughly circular vesicular core approximately 1 mm in diameter, surrounded by an opaque rim of about 100 μm average width and fractured quartz grains. The core was largely isotropic with a few crystalline fragments near the center. The core was covered by four grid openings of the copper support: locations studied in detail were in the third and fourth grids, shown optically in detail in Figure 15b, c, and d. During the ion-thinning process, many holes developed by enlargement of vesicles in the glass.

Electron Microscope Observations

Quartz. A few regions of relatively undeformed quartz with normal dislocation density remain in the Class 4 rock. Most of the quartz contains glass lamellae and a reduced dislocation density (Fig. 16a). In the sequence of shocked Coconino Sandstone from Class 2 to Class 4, dislocations in quartz were observed either to retain initial dislocation density (about 10^8 cm^{-2}) and configuration as found on relatively unstrained fragments, or to be absent, as in the strained quartz associated with glass lamellae. Excess dislocations above the initial density were *nowhere* observed whereas slow deformation has been observed to produce dislocation densities up to 10^{12} cm/cm^3 (Ardell et al., 1973). Also, there was

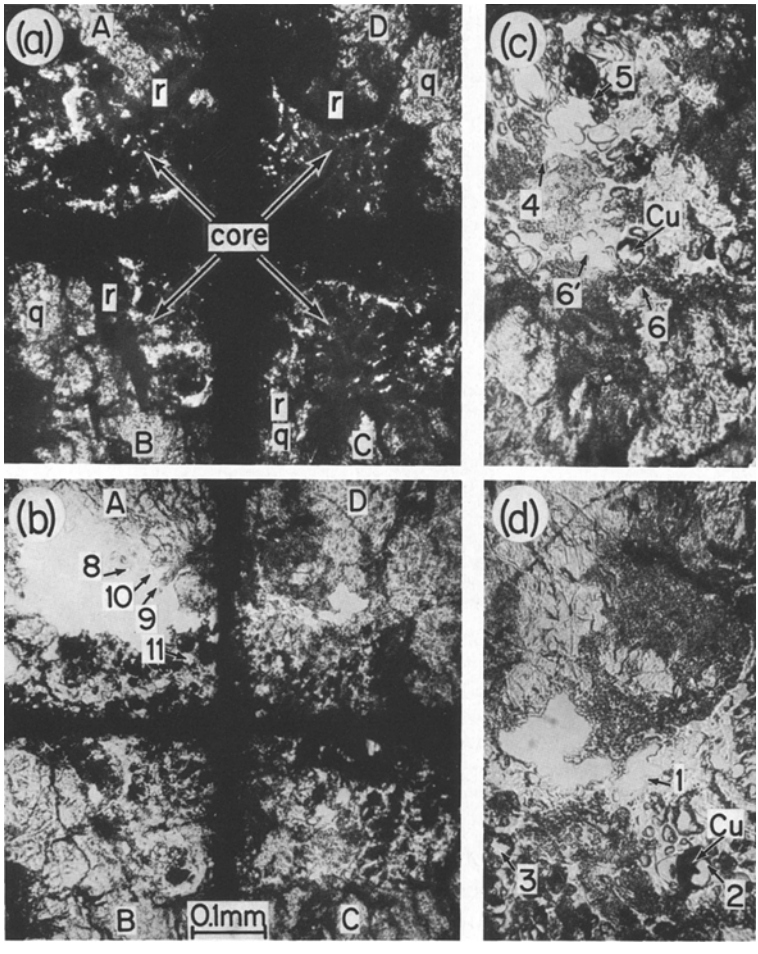

Fig. 15a–d. Optical photographs of Class 5 Coconino Sandstone Sample 17 used for TEM study. **a** The region in plane polarized light. **b** The region after ion thinning. A roughly circular core containing the high pressure phases is centered under the grid bar intersection in the center of the photos. By comparing (a) and (b), note the disappearance of opacity in parts of the previously opaque rim with thinning. Of the four grid openings covering the core and labeled A, B, C, D, we studied regions in grids A, C and D. Grids C and D are shown in photos (c) and (d). Because the thinned sample was extremely delicate, we were not able to obtain all photos of the thinned sample in the same orientation as the unthinned sample. **c** Enlarged view of part of Grid C of the ion-thinned sample, plane polarized light. This photo is mirrored about a vertical plane from (b). **d** Enlarged view of part of Grid D after ion thinning, plane polarized light, inverted from the orientation of photo b. Locations of the electron micrographs are indicated by the numbers in (b), (c) and (d). Some of the vesicles, such as the one labeled "Cu", are lined with black material. In two of these holes we determined that this material was copper by using an electron microprobe. This copper must have been sputtered from the grid bars onto the sample during ion-thinning

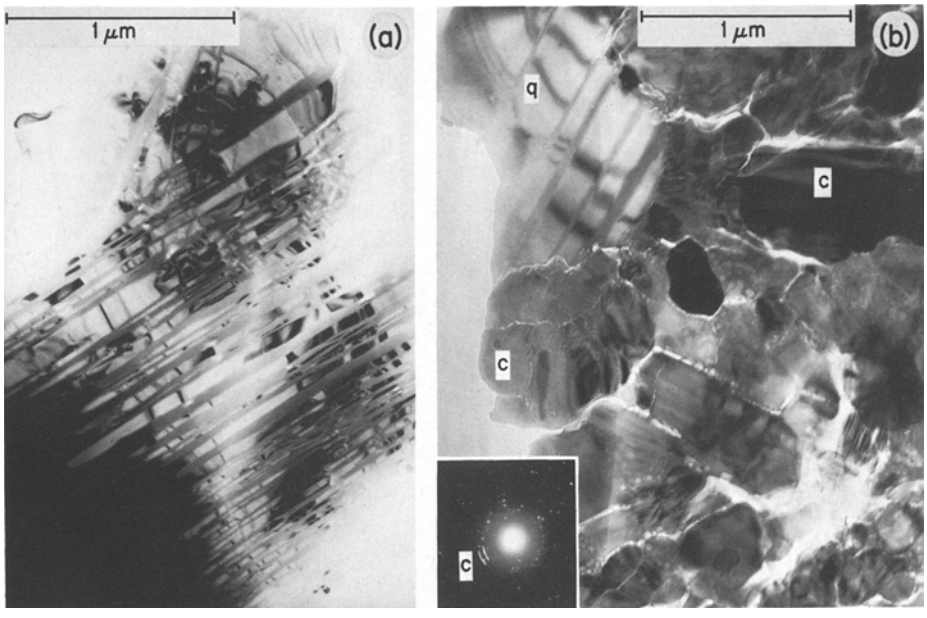

Fig. 16a and b. Electron micrographs of quartz and coesite in Class 4 Coconino Sandstone. **a** Quartz grain with parallel bands of glass; no diffraction pattern obtained. **b** Quartz grain "q" in direct contact with twinned coesite crystals "c", region 10 in Grid A on Figure 15. Small round vesicles occur on the boundaries of most of the coesite grains, probably in a thin amorphous rim. In places the vesicles have coalesced along glassy grain boundaries to form small cracks. The selected area diffraction pattern shown was taken with an aperture that covered the quartz grain in the upper left and adjacent coesite and shows a mixed pattern

no evidence for creation of dislocation tangles, cell walls or subboundaries. Our observations show that sites where the local degree of deformation is highest, namely, the regions around the dislocations, have been selectively removed by the shock process. We believe that the nucleation of glass lamelle takes place on such sites and on individual dislocations which are regions of stress concentrations.

Alternating quartz and glass lamellae are found in all classes of rocks, but generally are more abundant in the more highly shocked rocks. The glass occurs as parallel bands, up to 500 Å thick, alternating with layers of crystalline quartz. The bands frequently exceed one micron in length. The quartz slices are generally somewhat thicker than the glass slices and may show considerable strain contrast, indicating bending of the structure between glass layers. The quartz is generally free of dislocations when mixed with these glass bands. Diffraction patterns taken across mixtures of glass and quartz lamellae show some splitting of the spots and/or asterism, indicating misorientations of individual fragments on the order of a degree, and a glass halo caused by scattering from the amorphous layers.

Analyses of the traces of the lamellae in micrographs of regions of known orientation (determined from the diffraction patterns) show that some of the bands are parallel to the unit rhombohedra $\{10\bar{1}1\}$ and $\{10\bar{1}3\}$, an orientation characteristically seen in optical "planar features" (Bunch and Cohen, 1964).

These authors studied shock produced cleavages and found that they occur, in order of decreasing abundance, parallel to r{10$\bar{1}$1} or z{01$\bar{1}$1}, c{0001}, m{10$\bar{1}$0} or a{11$\bar{2}$0} and s{11$\bar{2}$2}, in general agreement with the crystal planes in quartz that require the least breaking of Si-O bonds {r, m, c, a, s, x} (Fairbairn, 1939). Optical planar features previously have been reported to be of a glassy nature (von Engelhardt et al., 1968, p. 475; Bunch, 1968, p. 413; Carter, 1968, p. 453). TEM observations of alternating bands of quartz and glass have previously been reported by Müller (1970) in experimentally shocked quartz. It is clear that the fine-scale glass lamellae observed with TEM are identical to the optically identified "planar features", except that they are commonly so closely spaced that they could not be resolved optically. The presence of unresolvable glass lamellae would, however, lower the index of refraction of the host grain and thus account for the anomalously low indices of refraction observed for shocked quartz grains (Stöffler, 1974).

The structure of "deformation lamellae" and "planar features" in quartz deformed experimentally in static experiments or by shock is a confused subject that is still under study by TEM. The perfectly basal deformation lamellae in experimentally deformed dry quartz originally interpreted as arrays of dislocations locked in the slip planes (Christie et al., 1964) were shown in some cases to be associated with thin basal Brazil twins and arrays of dislocations (McLaren et al., 1967) and subsequently thin zones of glass, also associated with arrays of dislocations (Christie and Ardell, 1974). The basal lamellae in the Jeppestown Sandstone, generally attributed to shock deformation (e.g. Carter, 1965), are more variable and complex in structure, consisting in some cases of simple dislocation arrays and in other cases planar defects and fine linear defects (Phakey and Christie, unpublished). Deformation lamellae in naturally deformed quartzites and in experimentally deformed synthetic quartz are also very variable: they are related to variable densities of dislocations in zones subparallel to the dominant slip planes, in some specimens zones of higher dislocation density (Boland et al., 1971) and in others recovered zones of lower dislocation density (Christie and Ardell, 1974); stress-optical effects due to the dislocation distributions are sometimes clearly responsible for the optical signatures of such lamellae. However, it is evident from our TEM studies of the shocked Coconino Sandstone, rocks from the Ries crater (Phakey and Christie, unpublished) and TEM studies of lunar breccias (Christie et al., 1973; Heuer et al., 1974; Nord et al., 1975) that the optically symmetrical "planar features" observed in shocked quartz and feldspars consist simply of microscopic or submicroscopic layers of thetomorphic glass and are not associated with dislocation arrays.

Opaque regions. Remnants of quartz grains in the Class 4 rocks are rimmed by opaque regions which contain polycrystalline coesite in a matrix of glass. Quartz-coesite contacts are observed (Fig. 16), as are glassy quartz-coesite contacts. The optically opaque regions are composed of irregularly shaped grains of coesite, approximately one-third micron in diameter (Fig. 16b). Amorphous material containing spherical bubbles surrounds many of the coesite grains. The bubbles, which are generally less than 100 Å to 500 Å in diameter, coalesce along some grain boundaries to form subparallel elongated fissures up to 0.1 mi-

cron in width and several microns in length (Fig. 16b). These cracks and vesicles cause the opacity. We have carefully compared TEM observations of cracks and vesicles with optical microscope and hand-specimen features to satisfy ourselves that the features described are not artifacts of the ion-thinning process.

Glass. The isotropic core is composed of vesicular glass (Fig. 17a) in which remnants of single-crystal coesite grains are embedded (Fig. 17b). The glass may be free of vesicles over areas up to about 5 μm diameter or may be densely populated with spherical or oblate vesicles ranging in size from several hundred Angstroms to several microns (Fig. 17a). Fragments of crystalline coesite which are embedded in the vesicular glass maintain single-crystal orientation over areas greater than 10 μm^2 (Fig. 17b). These single crystals of coesite may be the largest crystals of a high-pressure phase known to have been produced under shock conditions. We infer that at one time during the shock event large single crystals of coesite existed in the region now seen as the glass core. The crystals have subsequently inverted partially to glass. Since the coesite crystals retain their original outlines and traces of original texture, they satisfy one criterion for being "thetomorphic" (Chao, 1968). However, these "thetomorphic" grains occur in a mass of vesicular glass and show evidence of some misorientation in their diffraction patterns.

A gradational transition between thetomorphic glass and shock-melted lechatelierite frequently occurs over distances of a fraction of a micron, as in Figure 17b. This gradational type of transition also occurs in plagioclase grains in naturally shocked basalt from Lonar Crater, India (Kieffer, 1975b, 1976). In both the Lonar basalt and the Coconino Sandstone suites, thetomorphic glass grades into shock melted glass only in the more highly shocked rocks. A reasonable inference from this observation is that shock melting follows the formation of thetomorphic glass in the more highly shocked rocks.

We suggest that in rocks are shocked to high pressures and temperatures the textural distinction between thetomorphic glass and lechatelierite disappears and that the origin of the glass may not be inferred simply from the texture. Flow features, schlieren or vesicles, depend on the presence of water and on the viscosity of the material during glass formation. We feel that the *absence* of flow features is alone not sufficient evidence to preclude liquidus melting for the following reasons: The viscosity of pure silica is extremely high, but decreases with increasing temperature—typical values are 4.7×10^{13} poises at 1,100°C to 10^{10} poises at 1,440°C (Volarovich and Leontieva, 1936). The presence of water within silica would also diminish the viscosity. However, Uhlmann, Hays and Turnbull (1966) have concluded that available data on network liquids suggest that viscosity *increases* significantly with pressure, the amount of increase being less at high temperatures than at low temperatures. (For B_2O_3 glass, a structural analog to SiO_2 glass, at 359°C, the viscosity at 1 kb is 4.5 times the viscosity at 1 bar.) Thus, the effects of pressure and temperature on viscosity oppose each other. Although the existence of flow features may be taken as positive evidence of liquidus melting (possibly at much lowered temperatures of water is present), their absence is not definite evidence for the lack of liquidus melting, for viscosity and stress conditions may not have been conducive to flow.

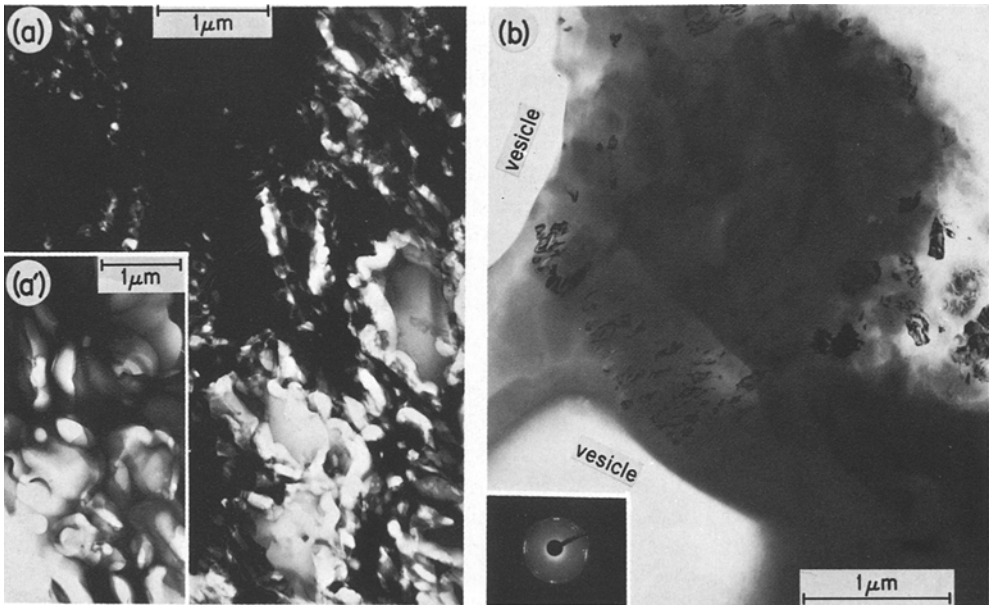

Fig. 17a and b. Electron micrograph of glass in Class 4 Coconino Sandstone. **a** Amorphous material containing large spherical or elliptical vesicles, region 6 in Figure 15c. **b** Fragments of coesite embedded in lechatelierite, region 1 in Figure 15d. The diffraction pattern shows that crystal fragments retain excellent single-crystal orientation; the zone axis is [011], [110] or [111]. We interpret a relationship such as this as evidence that the glass formed from a large (> 5 μm) preexisting coesite crystal

The electron microscope observations have provided criteria for the presence or absence of flow not available from optical work. Diffraction patterns taken across regions of glass containing crystalline fragments indicate that orientations of the fragments range from nearly single-crystal orientation to polycrystalline orientation. A diffraction pattern showing a nearly single crystal orientation of the remnant fragments (such as Fig. 17b) indicates that no significant amount of flow has occurred, for misorientations on only a few degrees are easily detected. A more strongly misoriented or polycrystalline pattern (such as Fig. 6a or 10d, e) indicates rearrangement of the crystalline domains which may be attributed to flow.

In summary, in Class 4 rocks, glass is formed primarily by melting of the high-pressure, polymorph, coesite, perhaps with thetomorphic coesite glass formed as an intermediate phase. Lesser amounts of glass are present as thetomorphic polymorphs of quartz and coesite. We did not find any evidence in these rocks that lechatelierite is formed by direct melting of quartz or by melting of stishovite.

7. The Origin of Glass and the Role of Water in Shocked Coconino Sandstone

The various phase relations and inferred transition paths for production of high pressure phases and glass observed in the Coconino Sandstone are sum-

marized schematically in Figure 18. A large amount of glass is produced in an impact event, some in a melt zone surrounding the meteorite and a substantial amount in localized places in partially melted rocks. In this section we examine the origin of these various kinds of glass.

We have used three criteria discussed in Section 6 to characterize three distinct types of amorphous material in the rocks. The three criteria are: (a) the presence or absence of schlieren and vesicles, (b) the nature of the electron diffraction patterns, and (c) characteristic textures. The three types of glass recognized are: (1) thetomorphic glass, (2) froth, and (3) lechatelierite. These three types of glass appear to have originated by different processes and at different times within the shock event.

(1) *Thetomorphic glass* occurs in the Class 2, 3 and 4 rocks as lamellae or domains in both quartz and coesite as hosts. Diffraction patterns taken across the glass and crystalline lamellae are usually single-crystal patterns showing misorientation, but, in nearly totally vitrified regions, the diffraction patterns are nearly polycrystalline because large misorientations of the crystal fragments occur. Thetomorphic glass was not observed in core coesite; this absence is significant and is considered in a later section. We do not find any evidence that thetomorphic glass lamellae in quartz are produced by reversion of a high pressure phase, as suggested by DeCarli and Jamieson (1959) and Stöffler and Hornemann (1972).

(2) *"Froth"* containing fine angular vesicles which have diameters as small as tens of Angstroms occurs only in Class 3 rocks. It is confined to thin surface layers ($\leqq 1$ μm) on host grains in or near the regions containing high pressure phases. The most prominent characteristic of the froth is the delicate nature of the walls of the small vesicles, from which we infer that the froth was emplaced late in the shock event, since the thin walls of such vesicles could not withstand compression. This froth is distinct from the lechatelierite found in abundance in Class 4 rocks.

The cryptovesicularity of the froth and the irregularity of the vesicle shapes suggest that it was produced by the violent separation of a gas phase from a liquid phase ("fritting"), and that this reaction was quenched in a short time. We suggest water for the gaseous, vesicle-forming phase and amorphous silica as the only possible constituent of the bubble walls. The water was available as pore water in the Coconino at the time of the formation of Meteor Crater (Shoemaker, 1960). The tendency of water to dissolve silica at high pressure and temperature was demonstrated by Kennedy et al. (1962). For example, at 9.5 kb and 1,050° C, water vapor in the system SiO_2-H_2O may contain over 60 percent by weight SiO_2.

The froth occurs predominantly in or near the regions containing high pressure phases. These regions containing the high pressure phases are the walls of collapsed pores (Kieffer, 1970, 1971). It is quite clear from thin section relationships that the froth did not originate outside the high pressure phase regions (i.e. outside of the ex-pore regions) because the veins are not so extensive. We therefore conclude that the froth was formed from material (water and silica) near the pore regions in the unshocked rocks.

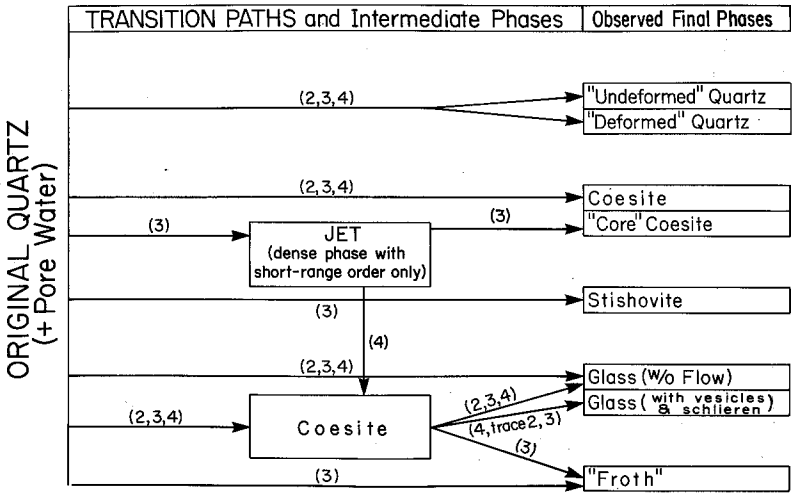

Fig. 18. Phases observed in Classes 2, 3 and 4 Coconino Sandstone and inferred transition paths

(3) *Lechatelierite* is distinct from froth because it contains predominantly spherical vesicles with dimensions on the order of hundreds of Angstroms and larger and occurs in regions larger than or comparable in size to the original grain size of the rock. It exists in abundance in Class 4 rocks and in only minute amounts in Class 2 and 3 rocks.

Vesicles in the lechatelierite are due to the exsolution of water from a supercritical SiO_2-H_2O mixture upon release of high pressure (Kieffer, 1971). The size and number of vesicles formed depends upon many factors such as rate of cooling and diffusion of vapor. Another important factor on which the extent of gas coming out of solution depends is the degree of supersaturation. High gas content is conducive to the formation of large numbers of very fine vesicles while a low gas content encourages much larger but fewer vesicles. The spherical shape of the vesicles in lechatelierite is a characteristic minimum surface energy configuration of bubbles in a glassy matrix. The existence of such a configuration may be regarded as evidence that the exsolution of water from the melt was not quenched, but occurred for some time.

The properties of both the froth and the lechatelierite indicate that water played an active chemical role and interacted with the SiO_2 minerals during the shock process. It cannot be regarded as an inert, isolated component. Although this interaction appears to be insignificant in considerations of shock processes on the lunar surface because of the dryness of the environment, it may be an important phenomenon in natural terrestrial cratering events, and in nuclear explosion processes. In the explosion experiments water is frequently present in target material and is known to affect the cratering efficiency of the explosion, not only by weakening the rocks, but by altering shock and particle velocities (Cherry and Petersen, 1970; Terhune et al., 1970; Higgins and Butkovich, 1967). Butkovich (1971) has proposed a cratering model which accounts to some extent for the influence of water on nuclear explosion events. This model, called the "water-boost model", predicts the cavity radius and

free surface velocity for cratering events with significantly better accuracy than models which ignore the presence of water. The water-boost model treats wet rocks as systems composed of two *noninteractive* components for the purpose of calculating the equation of state, e.g., the release path from a given pressure in the two-component system is calculated from the measured or calculated release path of each component, weighted by the fractional percentage of the component. Melting or phase changes in either the rock or water are included in the macroscopic behavior of the release P-V path for the individual components, but chemical interaction between the two components is not considered.

Our interpretation of the textures in moderately and strongly shocked Coconino suggest that there are at least three ways in which chemical interactions between silica and water occur in shock waves: (1) In rocks shocked to moderate pressures, water vapor dissolves and redeposits silica, producing the froth, upon release to low pressure. This interaction does not involve much of the rock component by mass, but could greatly affect the volume-expansion of steam at low pressures by trapping the water vapor in small holes in the frothy network. (2) In rocks shocked to high pressure water and silica form a supercritical mixture in which water is incorporated into silica melt. The dissolved water subsequently evolves to form vesicles after solidification has started. This process would alter the P-V release properties of the system, compared to one in which steam expands in noninteracting environment. (3) Water may substantially lower the melting point of grains with which it is in contact and may promote phase transitions by hydrolyzing Si-O bonds. (Since grain boundaries are the regions where most phase changes are initiated during the shock process, the phase changes are occurring in close proximity to pore water.) It is unlikely that melting and phase changes in a rock-water system will occur at the pressures and temperatures appropriate to the isolated rock component.

8. Pressure and Temperature Conditions

Pressure and temperature conditions in the naturally shocked rocks can be inferred only if the texture of these rocks can be compared to the texture of rocks recovered from laboratory experiments in which they have been shocked to known pressures and temperatures. Such comparison is not straightforward because, first, the necessary experiments have not been performed and, second, the duration of the impact event at Meteor Crater was more than 10,000 times the duration of a typical laboratory event. Since many of the phase changes described are very sluggish, a marked difference in the behavior of materials under shocks of two different durations may occur.

An assignment of pressures to the shocked Coconino sandstone samples was made by Kieffer (1970, 1971) on the basis Hugoniot data for *dry* quartz and *dry* Coconino Sandstone. In the following section these data are reviewed and are supplemented by Hugoniot data for water and wet NTS playa material, since we now believe that pore water was chemically active during the shock process. In addition, we discuss the phase diagrams and solubility data of Kennedy et al. (1962) and Ostrovsky (1966) for the SiO_2-H_2O system. We then use these laboratory data and our TEM observations to formulate a model for shock propagation through wet porous materials in Section 9.

Equation-of-state data for single-crystal quartz are summarized in Figure 19a (Wackerle, 1962; Ahrens and Rosenberg, 1968; Fowles, 1961). The shock data can conveniently be divided into three regimes. In Regime 1, material is compressed by elastic waves. Pressures in this regime range up to 35 to 50 kb for x-cut quartz and up to 80 to 130 kb for z-cut quartz. Wackerle estimated temperatures less than 200° C at 130 kb. Between 130 and 377 kb, in Regime 2, the shock-compressed volume of quartz is less than the volume of quartz compressed isothermally. It has been proposed (Ahrens and Rosenberg, 1968) that a mixture of phases is formed in this region: quartz and stishovite, or possibly quartz, coesite, and stishovite. At pressures above 377 kb, in Regime 3, quartz appears to be completely converted to a denser high-pressure phase. Since it is impossible to attain the large compression shown in the equation of state with bulk modulus and bulk modulus derivatives of normal crystalline materials, it is assumed that the compression indicates that a phase change has occurred in which silicon enters into six-fold coordination at high pressure. Measurements of the transient flow field in Arkansas novaculite shocked to 150 to 400 kb by Grady et al. (1976) suggest that the collapse to a dense phase occurs on a time scale substantially less than 0.035 μs. If the phase transformation continues after the initial shock loading, the rate is at least three orders of magnitude lower than the initial transformation rate in the shock front. Therefore, for all practical purposes, the phase change from quartz to the dense phase may be described as "instantaneous".

Six regimes (A-F) were described for the shocked dry Coconino Sandstone data by Kieffer (1971). These regimes are shown in Figure 19b and are summarized in Table 2, in which estimates of the average temperature conditions made by Ahrens and Gregson (1964) are included. The estimated temperatures shown in Table 2 are shock temperatures; because most of the energy is *P-V* work of compression of the pores and is nonrecoverable, these temperatures are also believed to represent *approximately* the average release temperatures. Local temperatures may be twice these values because of heterogeneity characteristic of shock conditions in porous media (Kieffer, 1970, 1971). The equation of state of shocked Coconino Sandstone shows a region of great compression above 300 kb. The compressed density indicates that silicon has entered into six-fold coordination.

The degree of crystallinity of the phase in six-fold coordination in the porous and nonporous samples has been the subject of some controversy. The strongest evidence that supports the argument that *crystalline* stishovite is formed is that traces of crystalline stishovite have been recovered from experimentally shocked quartz and sandstone by DeCarli and Milton (1965) and Kleeman and Ahrens (1973). Since the amount of stishovite recovered represents only a small fraction ($\ll 1\%$) of the original quartz, it is necessary to assume that, if stishovite were formed as postulated, most of it inverted to glass upon pressure release, perhaps because of instability of stishovite under high-temperature conditions. The fact that the release adiabat centered at 380 kb (Fig. 19a) shows substantial expansion at low pressure is interpreted as the inversion from six-fold to four-fold coordination (Ahrens and Rosenberg, 1968). On the other hand, we have seen *no* evidence for such an inversion of crystalline stishovite to glass in the TEM studies. The stishovite which we observed was wholly crystalline

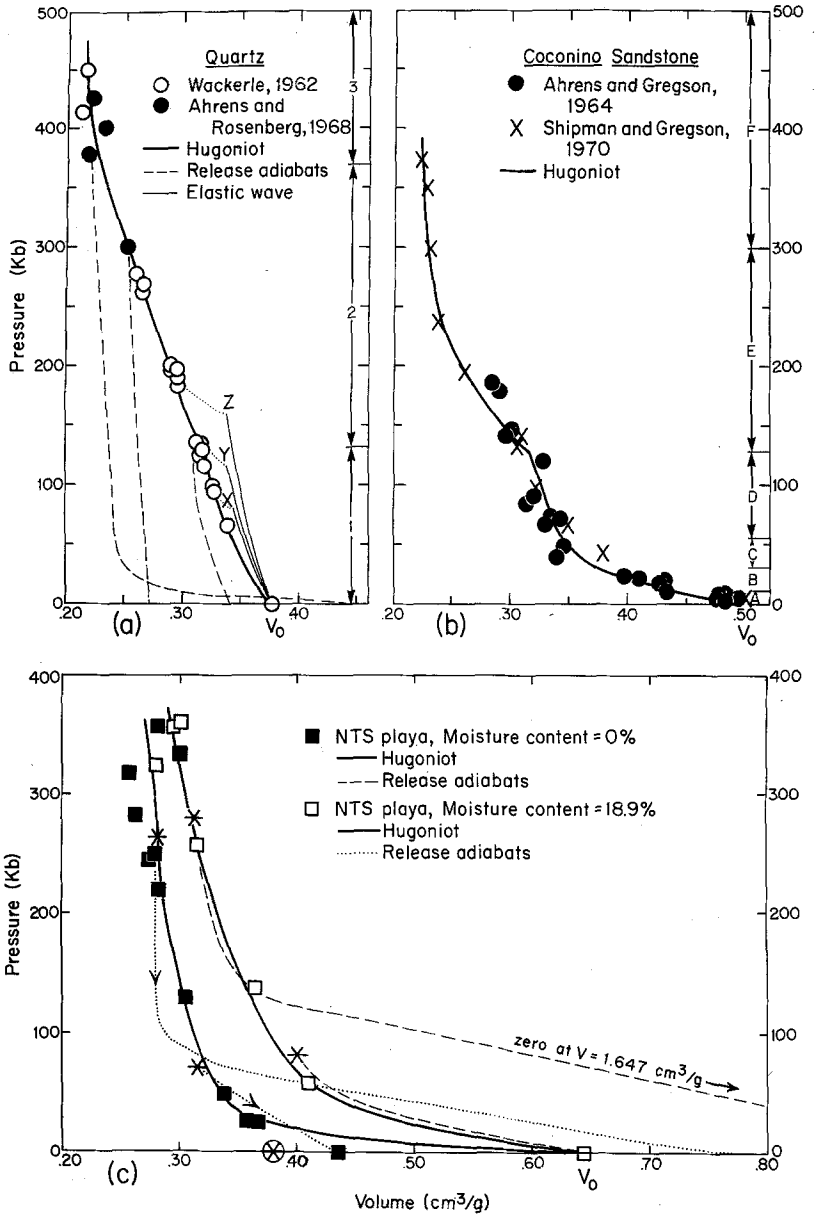

Fig. 19a–c. **a** The shock Hugoniot (heavy, solid curve) for single-crystal quartz. The light lines labeled x, y and z show the elastic, first-wave compression for waves propagated along the x, y and z axes respectively. Light dashed lines are release adiabats. Regimes 1, 2 and 3 shown on the right margin are discussed in the text. Data are from the sources shown. **b** The shock Hugoniot for Coconino Sandstone, showing on the right margin the six regimes A–F described in Table 2. **c** The Hugoniots (heavy lines) and release adiabats (light dotted and dashed lines) for wet and dry Nevada Test Site material of initial density 1.55 g/cm^3

Table 2. Regimes of the coconino sandstone hugoniot

Temperature	Regime	Pressure range[a]	Phenomena/Interpretation
~ambient	A	0 to 2–9 kb[b]	Elastic deformation. Very little grain damage
< 250° C	B	2–9 to 30 kb (22–45 kb)	Volume of compressed sandstone greater than the zero-pressure volume of quartz, 0.377 cm^3/g. Pores are present in the compressed state
< 350° C	C	30 to 55 kb (36–130 kb)	Volume of compressed sandstone less than initial volume of quartz and approaches the volume of shocked single-crystal quartz at higher pressures. Porosity is reduced to zero
350°–~ 950° C	D	55 to 130 kb	Sandstone Hugoniot follows closely single-crystal quartz Hugoniot. Possible formation of small amounts of coesite
> 1,000° C	E	130 to 300 kb	Volume of shocked sandstone less than volume of shocked quartz. Release adiabat data indicate that high-pressure phases are present in single-crystal quartz shocked to these pressures
	F	> 300 kb	Compressed density is appropriate to shocked dense phase. Release adiabats of single-crystal quartz suggest that grains shocked above 350 kb melt to fused silica on release

[a] Possible extreme values for upper limits as interpreted by Ahrens and Gregson (1961) and Shipman et al. (1970) are given in parentheses

[b] These pressures are "equilibration pressures", as the term was used in the discussion of the one dimensional model in Kieffer (1971). Peak pressures in individual quartz grains may be significantly greater

and was not related to the glass-bearing areas. In general, glass in the shocked Coconino Sandstone is formed by the inversion or melting of coesite, not stishovite, as described in detail in the next section.

In general, the behaviour of the shocked Coconino Sandstone must be interpreted in terms of the equation-of-state for porous materials. However, since it appears that instantaneous destruction of the four-fold coordination of single-crystal quartz does occur at pressures above 300 kb, we use this pressure as a limit for the maximum pressure attained in those regions of the rocks where quartz still exists. The pressures in fact may have been substantially lower than 300 kb because high temperatures attained by multiple shocks and rarefactions could have allowed the transformation of quartz to proceed at lower pressures than inferred from single crystal data (Kieffer, 1971).

The shock behavior of wet material is shown in Figure 19c; however, an examination of the Hugoniot and release adiabat data of pure water shown in Figure 20 will aid in understanding the behavior of wet material. The Hugoniot data for water to 250 kb shown in Figure 20 were obtained by Rice and Walsh (1957). Release adiabats have not been measured, but those calculated

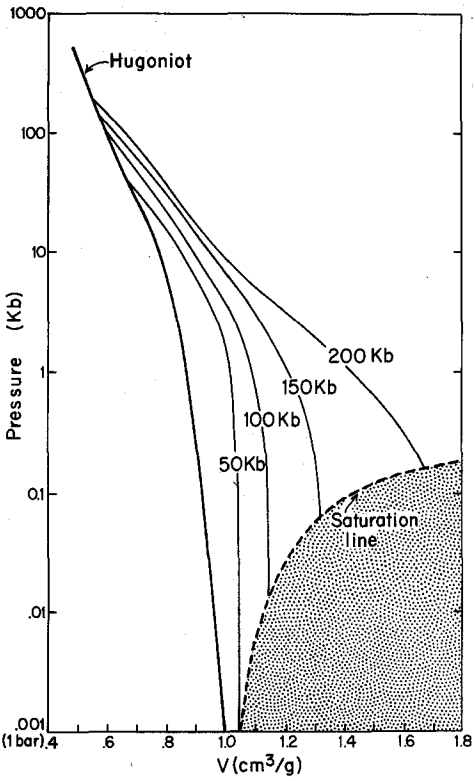

Fig. 20. The Hugoniot and calculated release adiabats (Riney et al., 1970) of water. At shock pressures greater than 50 kb, the release adiabats intersect the steam dome upon release

by Riney et al. (1970) from an assumed equation of state are shown. During release from shock states less than 50 kb, vaporization cannot occur because the internal energy retained upon decompression is insufficient to allow vaporization. At 100 kb shock pressure, however, the release adiabat enters the steam dome at approximately 10 bars pressure, and upon release from 150 kb, the material enters the steam dome at about 100 bars pressure (Riney et al., 1970). The pressure decay during rarefaction allows enormous expansion of the steam.

Shock and release data on wet sandstone are available only for pressures less than 12 kb (Murri and Smith, 1970). Therefore, in order to consider the high-pressure behavior of wet rocks, we show (Fig. 19c) Hugoniot and release data on wet and dry Nevada Test Site (NTS) playa material of initial density 1.55 g/cm^3 (Anderson et al., 1966). The wet material was 56 percent saturated. Since the densities of the wet and dry playa material were made equal, the actual pore volume was different for the wet and dry material. Although the playa material is not pure quartz, and although the porosity is not equivalent to the initial porosity of the Coconino, these data are quite representative of Hugoniot data obtained for dry and wet Ottawa sand, dry and wet Lebanon glycial till, and NTS playa sand of density near that of the Coconino, so we believe they illustrate the major shock phenomena characteristic of wet rocks.

The Hugoniot data of NTS material show a steepening at high pressure, duplicating the behavior of the dry Coconino (Fig. 19b). Since the NTS material is over 50 percent silica, it has been inferred from the resemblance of this Hugoniot to the quartz Hugoniot that the quartz in the sample transformed to a dense phase with silicon in six-fold coordination. The release adiabats from the high-pressure states in both the wet and dry material are steep initially and are generally interpreted to be the release adiabats of the high pressure phase (Fig. 19c). At lower pressures the release adiabats from the high-pressure states of the dry material flatten out and approach a density near that of silica glass. This behavior has been interpreted to reflect melting or inversion of the high-pressure phase. The release adiabat from the 280 kb state in the wet material (Fig. 19c) shows the initially steep decrease with pressure characteristic of the high-pressure phase, but then shows a large increase in specific volume at low pressure; there is considerable experimental uncertainty in the detailed form of this release curve. Anderson et al. (1966) attributed this expansion to vaporization of water and this interpretation is consistent with the behavior of water shown in Figure 20. It thus appears that the release path of strongly shocked wet materials is dominated by the behavior of water.

The Hugoniot data discussed above reflect the average, macroscopic behavior of shocked samples. On a microscopic scale the detailed response of the rock to the shock event must depend in a critical way on the initial composition—that is, on the ratio of silica to water — and on the pressure, temperature, and duration of the shock. A large number of shock and release histories are possible depending on the environments of individual grains. The final products and textures which are formed depend on the details of adiabatic release. In binary systems the thermodynamic behavior generally depends on the proportion of each component present. On a macroscopic scale, the ratio of silica to water in the Coconino Sandstone at the time of impact was probably large, even if water filled all of the initial pore spaces. On a microscopic scale, however, due to the short duration of the shock event, only a small fraction of the SiO_2 present was involved in SiO_2-H_2O interaction. For this reason, we feel justified in presenting the following discussion of a phase diagram based on data from a system of composition 50 percent H_2O–50 percent SiO_2 (Fig. 2a; Kennedy et al., 1962; Ostrovsky, 1966) and in using this phase diagram to interpret our results. We caution that shock conditions at Meteor Crater were not equilibrium conditions and we apply this discussion of the "equilibrium" phase diagram only in an attempt to understand *qualitatively* the behavior of the rocks and the general direction in which reactions would proceed to approach equilibrium.

Kennedy et al. (1962) examined the SiO_2-H_2O univariant melting curve and demonstrated that a critical end point exists at 9.7 kb and 1,080°C (Fig. 2a). The composition of the critical fluid at the critical end point is 75 percent by weight SiO_2 and 25 percent by weight H_2O. At high pressures and temperatures below the critical end point, water dissolves SiO_2, and Kennedy et al. report vapor phases with 60 percent by weight SiO_2.

The equilibrium phase data suggest that three possible conditions may exist in the SiO_2-H_2O system under shock conditions: (1) at low pressures and temper-

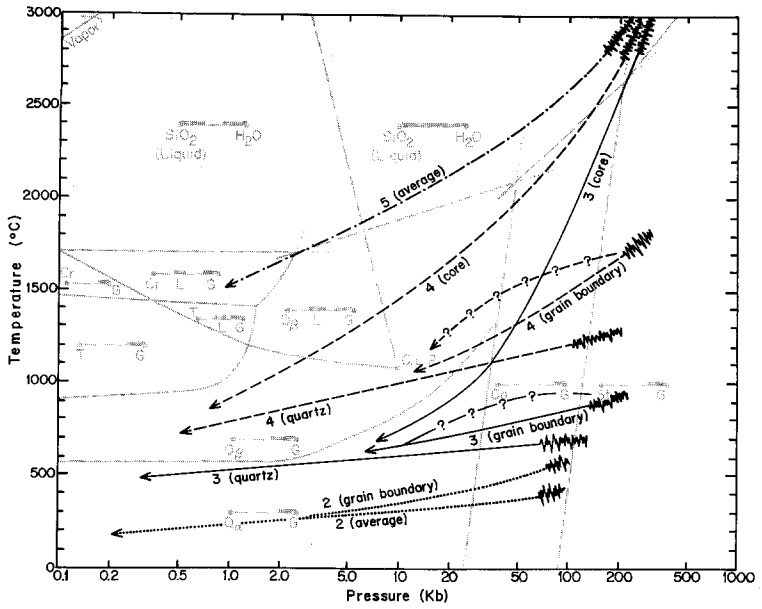

Fig. 21. Inferred pressure temperature release paths for different parts of shocked Coconino Sandstone, Classes 2, 3 and 4, superimposed on the SiO_2-H_2O phase diagram of Figure 2a. The curves show possible paths for grain boundaries, interior regions of quartz grains, Class 3 core coesite, Class 4 core glass, as well as "average" P–T conditions in the rocks. The Class 3 and 4 grain boundary curves shown with question marks show an inferred rise in temperature as the pressure decreases due to conduction of heat into a thermal aureole of fractured quartz surrounding the hot core material

atures, there may be no interaction between the silica and water and they may be considered as noninteracting components; (2) at higher pressures and temperatures, near the critical conditions, 1,080°C and 9.8 kb, silica may be dissolved in water vapor; (3) at pressures and temperatures above the critical conditions a supercritical SiO_2-H_2O fluid may be formed. The shock Hugoniot data allow an estimate of the pressures at which these conditions might be obtained: (1) In Class 2 rocks there is no evidence of silica-water interaction. Shock wave equation of state data indicate that such noninteracting behavior of water in a water-rock mixture is restricted to pressures below 100 kb. (2) In Class 3 rocks the "froth" appears to have originated from solution of silica by water vapor but water was not incorporated into silicate melt. We interpret this evidence to indicate that pore water was vaporized but that the critical end point conditions were not exceeded. Vaporization of water within rocks occurs if the average shock pressure has exceeded 100 kb. Final equilibration pressures were probably less than 250 kb in order to account for the amount of residual quartz in the rocks. At shock pressures greater than ~200 kb (from calculations based on water-tuff, not water-sandstone, mixtures), some part of the release state is above the critical end point for the SiO_2-H_2O system. (3) In Class 4 rocks there is evidence that water and melted silica were extensively intermixed over large regions, with subsequent exsolution of the water into

vesicles at lower pressures during release. Inferred pressure-temperature histories are shown schematically in Figure 21.

The *P-T* paths shown in Figure 21 illustrate the very large inhomogeneities of temperature that may have occurred in the rocks of each of the Classes 2, 3 and 4 on a submicroscopic scale. According to these inferred pressures and estimates of temperature, stishovite would be stable only in a narrow range of P-T conditions in wet rocks. It might form and exist at pressures as low as ~70 kb although the collapse to a dense structure has not been observed much below 150 kb in shock wave experiments. However, at pressures of only ~200 kb, shock temperatures in water-rock mixtures are great enough to cause a supercritical mixture to form. There is no indication that stishovite is formed under the supercritical conditions in the Coconino. Stishovite may therefore be rare in occurrence at Meteor Crater *not* because it inverted to glass, but because it could form only in a narrow range of pressures—with a lower bound set by transformation (nucleation and growth) kinetics and an upper bound determined by the SiO_2-H_2O critical conditions.

9. Shock Processes in Porous Quartzite

The following model of shock processes in porous quartzite is based on the observations of naturally shocked sandstones presented in this paper and in Kieffer (1971) and applies to impact events of relatively long duration, such as the Meteor Crater event. Many details of the model are given in the captions to Figures 22, 23 and 25 which illustrate the model schematically. In these figures, references to all of the plates discussed in the paper are shown by number in context of the model.

Weakly Shocked Rocks (Class 2: average pressure, $P \leqq 100$ kb). A weak shock wave propagating through a porous quartzite or granular quartz-rich soil compresses grains and collapses pores by shearing grains past each other along fracture surfaces (Fig. 22a, b). The most intense fracturing is confined to narrow rims along grain boundaries. As a result of the fracturing and compression, grains become elongated parallel to the shock front.

Even at relatively weak shock pressures thetomorphic glass may be formed within quartz grains, high pressure phases may form on grain boundaries and small amounts of melt may form locally, but many regions of the grains are essentially undamaged and retain their original fabric. High pressure phases nucleate and grow preferentially within the finely crushed quartz at grain boundaries. Melt is formed in regions of local stress concentrations. As the shock decays and the rarefaction passes, tensile stresses may exist, causing some of the coesite and quartz to invert to thetomorphic glass, and causing extension fractures to form late in the event (Fig. 22c, d). Water within pores is heated, but not appreciably vaporized, by a weak shock wave.

Moderately shocked rocks (Class 3: 100 kb $\leqq P <$ 200–250 kb). A moderately strong shock wave accomplishes pore closure by an entirely different process than a weak shock. In rocks shocked to pressures in excess of 100 kb, pores

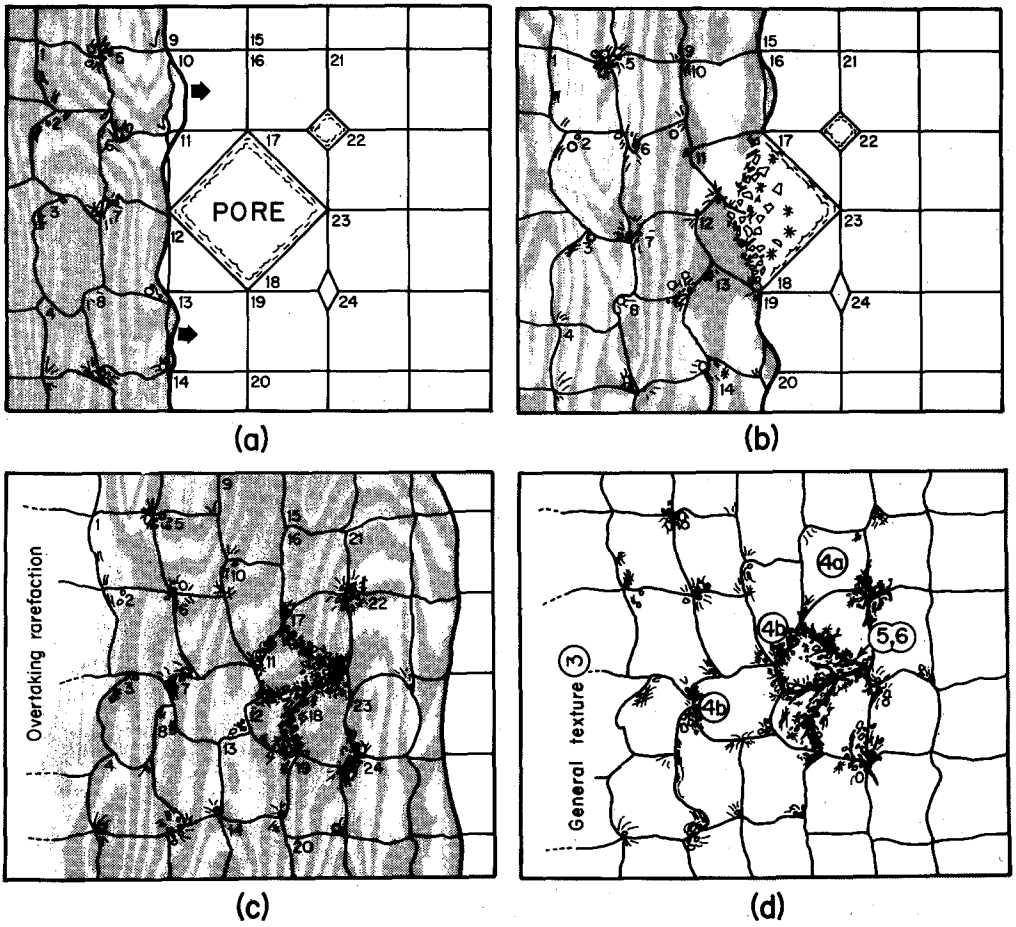

Fig. 22a–d. Schematic drawing of inferred shock history of a region containing pores in Class 2 Coconino Sandstone. Grains and pores have been given an arbitrary shape in order to make illustration easier. Small wavy lines within two of the three pores indicate initial pore water. Wood grain stippling schematically represents inhomogeneous shock and rarefaction structures. **a** The shock wave, as it approaches the water lined pore, is irregular in shape due to the many material inhomogeneities encountered in the rocks. Grains of the compressed region behind the shock have been rotated and sheared to fill cracks and pores. Fractured quartz (lines) and coesite nuclei (dark circles) have formed along the collapsed grain boundaries. **b** Pore collapse is accomplished by motion of grains around each other and into the pores. **c** Coesite nuclei grow into grains of about 1 μm diameter during the shock and in the rarefaction. **d** The coesite grains form symplektic veins on the edges of the quartz grains; many coesite grains and some quartz grains partially invert to thetomorphic glass

are filled with material *jetted* from the collapsing walls of pores (Fig. 23). A brief description of the theory of jetting as applicable to porous rocks has been given by Kieffer (1975).

Jetting is the extrusion of material at high velocities due to the impact of surfaces at oblique angles. The stream of hot material that emanates from the point of collision is referred to as the "jet" and the final products of

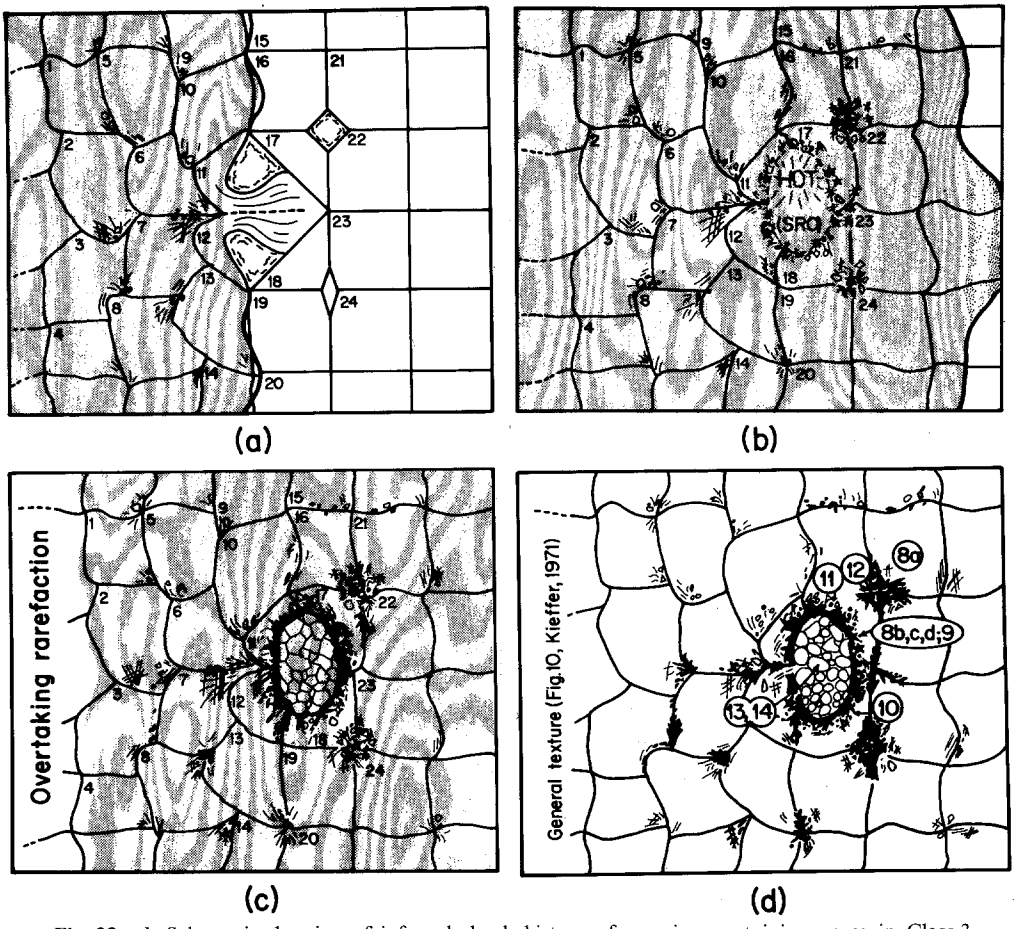

Fig. 23a–d. Schematic drawing of inferred shock history of a region containing pores in Class 3 Coconino Sandstone. See Figure 22 for general notation. Panel (a) of Figure 22 is not repeated in this Figure. **a** A jet is formed from collapsing grains and is injected into the pore. **b** A hot amorphous phase (SRO=short range order) existed temporarily in the collapsed pore. Stishovite (shown as stars) forms in regions of high stress. **c** Upon pressure release the jet cools to form a jectum consisting of coesite crystals which nucleate and grow to an equilibrium grain boundary configuration in the core. A thermal aureole forms around the jectum or collapsed pore as heat flows outward into the cooler quartz grains. The transformation of quartz to coesite is accelerated by high temperatures within the thermal aureole and results in the formation of an intimate intergrowth of quartz and coesite in the opaque rim. **d** At the end of the shock event hot water vapor circulates through cracks in the vicinity of the core, eroding SiO_2 from some grains and redepositing it elsewhere as froth. The eroded texture of the core coesite is shown schematically

the jetting process (cooled from high temperature) are referred to as "jecta" (Kieffer, 1975). The phenomenon of jetting has been known for nearly 150 years and was studied especially during and after World War II in connection with fabrication of shaped charges. Detailed considerations of experiments and of theory from a classical hydrodynamic viewpoint and from a shock wave model have been given by Birkhoff et al. (1948), Walsh et al. (1953), and Allen et al.

(1959). The phenomenon was recognized in simulated hypervelocity meteorite impacts of spheres onto planar surfaces by Gault et al. (1963).

Oblique angles of impact are required for jet formation (Fig. 24a). In the Coconino Sandstone, or in soils, the required oblique angles are provided by pore boundaries, irregular grain shapes, and imperfect grain fits. In order to explain the jetting process, it is useful to approximate the pores as collapsing wedges and cones (Fig. 24a), a geometry first considered by Birkhoff et al. (1948).

Jets arise only under certain specific conditions of impact (Walsh et al., 1953). In Figure 24b we show the approximate regions of jetless and jet-forming flow in aluminum from the data and theory of Walsh et al. (1953). Note that at a given impact velocity low-angle impacts are jetless. (The shock impedance properties of quartz are similar to those of aluminum and hence aluminum data can be used to provide order of magnitude estimates of the shock properties for jetting. A discussion of jetting and its occurrence in Class 3 Coconino Sandstone is given in Kieffer (1975b) and is not repeated here.)

The propagation of a moderately strong shock through a porous quartzite or quartz-rich soil is accompanied by jetting. The shock wave causes quartz grains to impact against each other as pores collapse (Fig. 22a). The leading regions of such grains are jetted into the pores (Fig. 23a, b), forming cores of molten material. The subsequent rarefaction history determines the final phase which crystallizes in the cores. Our textural evidence suggests that coesite, not stishovite, is the first stable crystalline phase in the cooling jet. The trailing regions of impacting grains do not enter the jets and are much less strongly shocked than the jet-forming material. These regions of the grains (plus other grains originally further from the pores) form a matrix of fractured material which surrounds the jecta (Fig. 23c, d).

The thermal histories of these various regions are shown in Figure 21. Since the microstructural relations suggest that stishovite is not formed in the core, the thermal history of a core region is shown by-passing the stishovite stability field. The thermal histories of the grains are, in comparison to the cores, relatively cold. However, the jets cool by conduction of heat into the surrounding matrix of cooler quartz, causing thermal aureoles to form (Fig. 23c). Some of the material within the aureoles may undergo phase changes accelerated by the high temperatures. In the Coconino Sandstone, these thermal aureoles are the opaque rims.

Estimates of the time scales for heat transfer may be made from the following simple model. A spherical jet of radius $a = 100\ \mu m$ and typical mineral thermal diffusivity, $\kappa = 0.01\ cm^2/s$, has a characteristic cooling time given by $\kappa t/a^2 \sim 1$ (Carslaw and Jaeger, 1959, p. 234). Pressure, temperature, and radiative dependences of the diffusivity are ignored in this estimate. This characteristic cooling time is approximately 10 ms. The jets will *not* cool significantly during the peak pressure pulse; however, a substantial amount of their heat *will* be transferred to the peripheral thermal aureole by the time that the pressure has decayed to the lower limit of the coesite stability field, 20 to 40 ms.

Grain boundaries receive more shock energy than grain interiors for two reasons: they are the foci of stress concentrations and they receive heat conducted

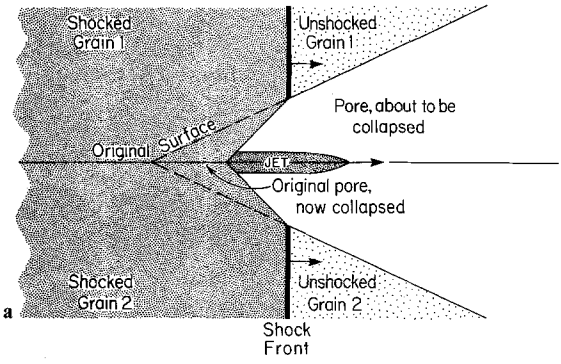

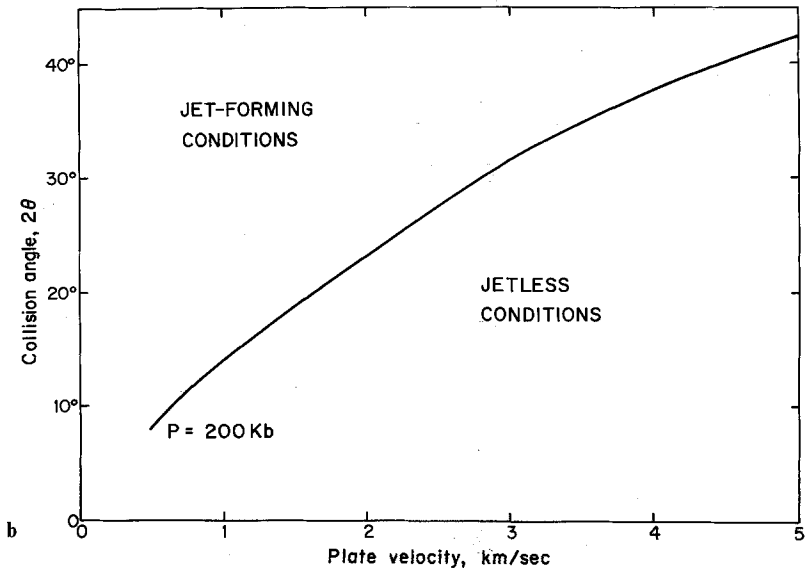

Fig. 24. **a** Shock wave patterns and surface collapse configuration of jetting wedge. Two grains surround the triangular pore. The shock front is in the process of collapsing the pore; material which has been shocked is shown in heavy stipple, material which is unshocked is shown in light stipple. The original surface of the pore is shown by the dashed line; the surface of the pore and the jet configuration after the shock has bassed are indicated. **b** Limiting conditions for jet formation as a function of impact velocity for aluminum. At low impact velocities, jets will be formed for all collision angles greater than 10–20°. At higher impact velocities, greater angles of impact are required for production of a jet

from jets. High pressure phases (coesite and stishovite in the Coconino Sandstone) grow directly from the original grains in these relatively warm regions. The growth of the high pressure phases can occur not only at the time of peak pressure, but also during decompression down to the lower limits of the stability fields of the high pressure phases, unless the temperature drops below values at which the transformations can proceed rapidly. The high pressure

phases which are preserved in the Coconino Sandstone are metastable and were preserved by quenching as the temperature rapidly decreased in the rarefaction.

The detailed shock history of pore water in the rocks is complex. During passage of a moderately strong shock, water is probably confined to the regions around collapsed pores, possibly in the form of high-pressure ice polymorphs. The holes, cracks and pores which are so prominent in the TEM micrographs of opaque and symplektic regions may reflect the location of the interstitial water during the compressive stage of the shock. Upon adiabatic release to low pressures, the water or ice expands violently to hot steam. The steam expands into fractures in and along grains boundaries of the SiO_2 phases, dissolving silica in places and redepositing it in others, depending on the local temperatures in the rocks. We consider that the froth observed in the regions of collapsed pores is formed by this process. The presence of this froth throughout the regions containing fractured quartz and high pressure phases reflects the motion of water vapor after passage of the main part of the shock. With shocks of moderate strength pore water does not interact with the silica jets or the jecta until very late in the rarefaction when vapor intrudes into microcracks in the jecta and interacts with the surfaces and corners of the coesite grains.

The absence of glass lamellae and thetomorphic glass in the core coesite was noted earlier and an attempt should be made to explain why such coesite does not form thetomorphic glass, as does the coesite which is inferred to have formed directly from quartz. We suggest the following explanation: The core coesite is the only phase in the rock which nucleates and grows from a denser phase (the jet, which at high pressure probably consists of silica in six-fold coordination). As coesite nucleates from this jet, it is constrained to grow in a volume determined by the *denser* phase and, hence, is effectively under a local confining pressure throughout the rarefaction part of the event. Thus tensile stresses, which we believe are associated with the formation of glass lamellae in other parts of the rock, may not be present in such regions.

It appears that stishovite is present only on the periphery of the core material. The stishovite which we observed in the samples is wholly crystalline, and shows no evidence of reversion to glass. We are forced to conclude that *only a small amount of stishovite was formed* in the rocks that we have examined from Meteor Crater and that *the stishovite that was formed is preserved.* The only other place where stishovite could have formed is in the cores and they show no textural or mineralogical evidence of the former presence of stishovite. Further observations on stishovite *in situ* in shocked Coconino Sandstone are necessary before a model for stishovite formation, growth, and possible destruction can be offered; these observations are difficult, however, because of the scarcity of stishovite and the difficulties of sample preparation discussed in Section 3.

Strongly shocked rocks (Class 4: $P > 200$ kb). The initial stages of pore collapse by a strong shock wave are similar to those of collapse by a moderately strong shock. For this reason, panels a and b of Figure 23 are not repeated in Figure 25,

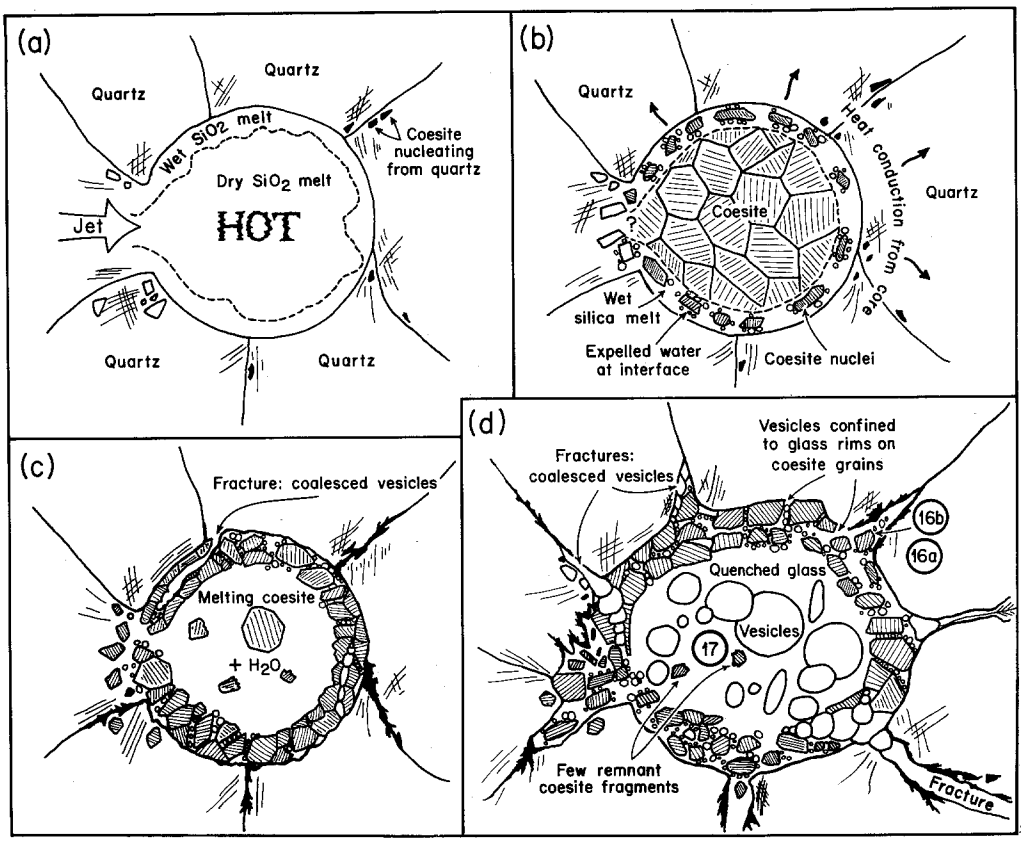

Fig. 25a–d. Schematic drawing of inferred shock history of a region containing pores in Class 4 Coconino Sandstone. See Figure 22 for general notation. Panel (a) of Figure 22 and Panel (a) of Figure 23 are not repeated in this Figure but show the early shock history of the pore schematically. **a** The hot jet is injected into the pore, forming a core of dry SiO_2 melt, probably surrounded by a rim in which SiO_2 and water are both present. **b** Coesite nucleates and grows up to 5 μm diameter in the central dry region, but to lesser diameter on the cooler perimeter. Water expelled from the wet perimeter is restricted to vesicles in glassy rims on the coesite grains. **c** Upon further decompression, the coesite in the core melts and the melt incorporates water available from the exterior regions. **d** The water subsequently exsolves from the melt, forming the abundant spherical vesicles observed in Class 4 rocks. Coalescence of the vesicles leads to the formation of fissures and fractures

which shows the final stages of the shock process in strongly shocked rocks.

During the passage of a strong shock wave, jets are injected into the pore spaces, forming hot cores which, we infer, are initially amorphous and have silica in six-fold coordination. Upon decompression through the coesite stability field during the rarefaction, crystals of coesite nucleate and grow in the interiors of the cores. These interior regions of the cores stay relatively hot during the evolution of the coesite; hence the crystals attain dimensions of over five microns. In the rims of the cores, which cool by conduction into surrounding quartz grains during the first few milliseconds of the shock, coesite crystals which grew from the melt are much smaller, rarely exceeding a micron in length.

The growth of coesite crystals from the SiO_2-H_2O melt causes concentration of water in the residual melt. Such a concentration of water into into small rims of melt on the coesite crystals is observed near the core boundaries (Fig. 20b).

Upon further pressure release the coesite in the centers of the cores begins melting. Water vapor becomes mobile and pockets of wet melt are formed in the core. Upon final cooling below critical pressure and temperature, the gaseous phase separates from the melt, forming myriads of vesicles within the glass.

It should be emphasized that the glass found in shocked Coconino Sandstone was formed by a complex multistage process of phase changes: jetting of quartz grains into pores, crystallization of coesite in the jets and, finally, melting of this coesite.

10. Concluding Comments

Rocks shocked to higher pressures than those examined here are totally converted to glass upon release and, hence, no record of processes occurring at pressures in excess of approximately 300 kb is available. However, the observations reported here clearly show that the detailed processes by which a porous rock collapses under shock compression are complex, and that it is *wrong* to assume simple collapse to a single homogeneous phase at high pressure. The heterogeneity inherent in an initially porous rock determines that heterogeneity will be present in the shocked state and in much, it not all, of the released state even for very high shock presures and very long shock events.

Acknowledgments. We thank A. Ardell for allowing use of the electron microscope and E.M. Shoemaker for his interest and support on NASA grant NGL-05-002-003. Parts of this work were sponsored by NSF GA 26027 and NASA NSG 7052. J. deGrosse prepared special sections from very difficult materials. V. Doyle-Jones contributed valuable ideas for the illustrations.

References

Ahrens, T.J., Gregson, V.G.: Shock compression of crustal rocks: data for quartz, calcite, plagioclase rocks. J. Geophys. Res. **69**, 4839–4874 (1964)

Ahrens, T.J., Rosenberg, J.T.: Shock metamorphism: experiments on quartz and plagioclase. In Shock metamorphism of natural materials. B.M. French and N.M. Short, Eds., pp. 59–85. Baltimore, Md: Mono 1968

Allen, W.A., Morrison, H.L., Ray, D.B., Rogers, J.W.: Fluid mechanics of copper. Phys. Fluids **2**, 329–333 (1959)

Anderson, G.D., Duvall, G.E., Erkman, J.O., Fowles, G.R., Peltzer, C.P.: Investigation of equation of state of porous earth media. Stanford Research Institute Tech. Rept. AFWL-TR-65-146, 176 pp. (1966)

Ardell, A.J., Christie, J.M., Tullis, J.A.: Dislocation substructures in experimentally deformed quartzites. Crystal Lattice Defects **4**, 275–285 (1973)

Birkhoff, G., MacDougall, D.P., Pugh, E.M., Taylor, G.: Explosions with lined cavities. J. Appl. Phys. **19**, 563–582 (1948)

Bohn, v., E., Stöber, W.: Coesit und Stishowit als isolierte natürliche Mineralien. Neues Jahrb. Mineral. Monatsh. **3**, 89–96 (1966)

Boland, J.N., McLaren, A.C., Hobbs, B.E.: Dislocations associated with optical features in naturally deformed quartz. Contr. Mineral. Petrol. **30**, 53–63 (1971)

Bunch, T.E.: Some characteristics of selected minerals from craters. In: Shock metamorphism of natural materials, B.M. French and N.M. Short, Eds., pp. 413–432. Baltimore, Md: Mono 1968

Bunch, T.E., Cohen, A.J.: Shock deformation of quartz from two meteorite craters. Geol. Soc. Am. Bull. **76**, 1263–1266 (1964)

Butkovich, T.R.: Influence of water in rocks on effects of underground nuclear explosions. J. Geophys. Res. **76**, 1993–2011 (1971)

Carslaw, H.S., Jaeger, J.C.: Conduction of heat in solids, second edit., 510 pp. London: Oxford Univ. Press, 1959

Carter, N.: Basal quartz deformation lamellae—a criterion for recognition of impactites. Am. J. Sci. **263**, 786–806 (1965)

Carter, N.L.: Dynamic deformation of quartz. In: Shock metamorphism of natural materials, B.M. French and N.M. Short, Eds., pp. 453–474. Baltimore, Md: Mono 1968

Chao, E.C.T.: Impact metamorphism. In: Researches in geochemistry, Vol. II. Ed. P. Abelson, pp. 204–244. New York: John Wiley 1967

Chao, E.C.T., Fahey, J.J., Littler, J., Milton, D.J.: Stishovite, SiO_2, a very high pressure new mineral from Meteor Crater, Arizona. J. Geophys. Res. **67**, 419–421 (1962)

Chao, E.C.T., Shoemaker, E.M., Madsen, B.M.: First natural occurrence of coesite. Science **132**, 220–221 (1960)

Cherry, J.T., Petersen, F.L.: Numerical simuation of stress wave propagation from underground nuclear explosions. Lawrence Radiation Lab. Rept. UCRL-72216, Livermore, Ca., 1970

Christie, J.M., Ardell, A.: Substructures of deformation lamellae in quartz. Geology **2**, 405–408 (1974)

Christie, J.M., Griggs, D.T., Carter, N.L.: Experimental evidence of basal slip in quartz. J. Geol. **72**, 734–756 (1964)

Christie, J.M., Griggs, D.T., Heuer, A.H., Nord, G.L., Radcliffe, S.V., Lally, J.S., Fisher, R.M.: Electron petrography of Apollo 14 and 15 breccias and shock-produced analogs. Proc. 4th Lunar science Conf. Geochim. Cosmochim. Acta, Suppl. 4, **1**, 365–382 (1973)

Christie, J.M., Heard, H.C., LaMori, P.N.: Experimental deformation of quartz single crystals at 27–30 kb. confining pressure and 24°C. Am. J. Sci. **262**, 26–55 (1964)

Coes, L.: A new dense crystalline silica. Science **118**, 131–132 (1953)

DeCarli, P.S., Jamieson, J.C.: Formation of an amorphous form of quartz under shock conditions. J. Chem. Phys. **31**, 1675–1676 (1959)

DeCarli, P.S., Milton, D.J.: Stishovite: synthesis by shock waves. Science **147**, 144–145 (1965)

Engelhardt, W.v., Hörz, F., Stöffler, D., Bertsch, W.: Observations on quartz deformation in the breccias of West Clearwater Lake, Canada, and the Ries Basin, Germany. In: Shock metamorphism of natural materials, B.M. French and N.M. Short, Eds., pp. 475–482. Baltimore, Md: Mono 1968

Fairbairn, H.W.: Correlation of quartz deformation with its crystal structure. Am. Mineralogist **24**, 351–368 (1939)

Fowles, G.R.: The development of an explosive electric transducer. Part 1: Equation of state of quartz. Final Report 18-1996-A for Sandia Corp., Livermore, Cal., 33 pp. (1961)

Frondel, C.: The systems of mineralogy. In: Silica minerals, seventh edit., Vol. 3, 334 pp. New York: John Wiley, 1962

Gault, D.E., Shoemaker, E.M., Moore, H.J.: Spray ejected from the lunar surface by meteoroid impact. NASA Technical Note D-1767, 39 pp. (1963)

Grady, D.E., Murri, W.J., DeCarli, P.S.: Hugoniot sound velocities and phase transformations in two silicates. J. Geophys. Res. **80**, 4857–4861 (1975)

Heuer, A.H., Firestone, R.F., Snow, J.D., Green, H.W., Howe, R.G., Christie, J.M.: An improved ion thinning apparatus. Rev. Sci. Instr. **42**, 1177–1185 (1971)

Higgins, G.H., Butkovich, T.R.: Effect of water content, yield, medium, and depth of burst on cavity radii. Lawrence Rad. Lab. Rept. UCRL-5023, Livermore, Ca., 1967

Heuer, A.H., Christie, J.M., Lally, J.S., Nord, G.L.: Electron petrographic study of some Apollo 17 breccias. Proc. 5th Lunar Science Conf. Geochim. Cosmochim. Acta, Suppl. 5, **1**, 275–286 (1974)

Hörz, F.: Statistical measurements of deformation structures and refractive indices in experimentally shock loaded quartz. In: Shock metamorphism of natural materials, B.M. French and N.M. Short, Eds., pp. 243–253. Baltimore, Md: Mono 1968

Holm, J.L., Kleppa, O.L., Westrum, E.F.: Thermodynamics of polymorphic transformations in silica. Thermal properties from 5 to 1070° K and pressure-temperature stability fields for coesite and stishovite. Geochim. Cosmochim. Acta **31**, 2289–2307 (1967)

Kennedy, G.C., Wasserburg, G.J., Heard, H.C., Newton, R.C.: The upper three-phase region in the system SiO_2-H_2O. Am. J. Sci. **260**, 501–521 (1962)

Kleeman, J.D., Ahrens, T.J.: Shock-induced transition of quartz to stishovite. J. Geophys. Res. **78**, 5954–5960 (1973)

Kieffer, S.W.: I. Shock metamorphism of the Coconino Sandstone at Meteor Crater, Arizona II. The specific heat of solids of geophysical interest. Ph.D. Thesis, 253 pp. Calif. Inst. of Technology, Pasadena, Ca. 1971

Kieffer, S.W.: Shock metamorphism of the Coconino Sandstone at Meteor Crater, Arizona. J. Geophys. Res. **76**, 5449–5473 (1971)

Kieffer, S.W.: From regolith to rock by shock. Moon **13**, 301–320 (1975a)

Kieffer, S.W.: Droplet chondrules. Science **189**, 333–340 (1975b)

Kieffer, S.W.: Shocked basalt from Lonar impact crater, India, and experimental analogues, to be published in Proc. Seventh Lunar Sci. Conf. (1976)

McLaren, A.C., Retchford, J.A., Griggs, D.J., Christie, J.M.: Transmission electron microscope study of Brazil twins and dislocations experimentally produced in natural quartz. Phys. Stat. Solidi **19**, 631–644 (1967)

Müller, W.F.: Stosswelleneffekte in den Mondproben. Umschau **11**, 331–335 (1970)

Murri, W.J., Smith, C.W.: Equation of state of rocks. Interim Technical Report for U.S.A.E.C., Lawrence Rad. Lab. Contract AT(04-3)-115, 139 pp. (1970)

Nord, G.L., Christie, J.M., Heuer, A.H., Lally, J.S.: North Ray Crater breccias: an electron petrographic study. Proc. 6th Lunar Sci. Conf. Geochim. Cosmochim. Acta, Suppl. **6**, 1, 779–797 (1975)

Ostrovsky, I.A.: P-T diagram of the system SiO_2-H_2O. Geol. J. **5**, 125–134 (1966)

Petersen, C.F., Erlich, D.C.: Dynamic properties of rock required for prediction calculationa. Final report prepared for Defence Nuclear Agency, Stanford Research Institute, 72 pp. (1972)

Ramsdell, L.S.: The crystallography of coesite. Am. Mineralogist **40**, 975–982 (1955)

Rice, M.H., Walsh, J.M.: Equation of state of water to 250 kb. J. Chem. Phys. **26**, 824–830 (1957)

Riney, T.D., Garg, S.K., Kirsch, J.W., Morland, L.W., Hastings, C.R.: Stress wave effects in inhomogeneous and porous earth materials. Systems, Science and Software Report 35R-267 (1970)

Rogers, A.F.: A unique occurrence of lechatelierite or silica glass. Am. J. Sci. **19**, 195–202 (1930)

Scherer, G., Vergano, P.J., Uhlmann, D.R.: A study of quartz melting. Phys. Chem. Glasses **11**(3), 53–58 (1970)

Sclar, C.B., Carrison, L.C., Cocks, G.G.: Stishovite: Thermal dependence of the erystal habit. Science **144**, 833–835 (1964)

Shipman, F.H., Gregson, V.G., Jones, A.H.: A shock wave study of Coconino Sandstone. Final Report MSL-70-14 prepared for NASA, General Motors Technical Center, Warren, Michigan 46 pp. (1970)

Shoemaker, E.M.: Penetration mechanics of high velocity meteorites, illustrated by Meteor Crater, Arizona. Rept. Intern. Geol. Congr., XXI Session, Norden **18**, pp. 418–434, 1960

Shoemaker, E.M.: Impact mechanics at Meteor Crater, Arizona. In the solar system, Vol. 4, The moon, Meteorites and comets, B.M. Middlehurst and G.P. Kuiper, Eds., pp. 301–336. Chicago: Univ. Chicago Press 1963

Smith, C.S.: Some elementary principles of polycrystalline microstructure. Met. Rev. **9**, 1–48 (1964)

Stishov, S.M., Belov, N.V.: Crystal structure of the new dense modification of silica. Dokl. Akad. Nauk SSR **143**, 146–148 (1962)

Stishov, S.M., Popova, S.V.: A new dense modification of silica. Geochemistry **10**, 923–926 (1961)

Stöffler, D.: Deformation and transformation of rock-forming minerals by natural and experimental shock processes. II. Physical properties of shocked minerals. Fortschr. Mineral. **51**, 256–289 (1974)

Stöffler, D., Hornemann, V.: Quartz and feldspar glasses produced by natural and experimental shock. Meteoritics **7**, 371–394 (1972)

Takahashi, T.: Factors influencing pressure in multi-anvil devices. In: High-pressure measurement, A.A. Giardini and E.C. Lloyd, pp. 240–245. Washington, D.C.: Butterworth 1963

Terhune, R.W., Stubbs, T.F., Cherry, J.T.: Nuclear cratering on a digital computer. Lawrence Radiation Lab. Rept. UCRL-72032, Livermore, Cal, 1970

Trueb, L.F.: An electron-microscope study of shock-synthesized diamond. J. Appl. Phys. **39**, 4707–4716 (1968)

Trueb, L.F.: Microstructural study of diamonds synthesized under conditions of high temperature and moderate explosive shock pressure. J. Appl. Phys. **42**, 503–510 (1971)

Uhlmann, D.R., Hays, J.F., Turnbull, D.: The effect of high pressure on crystallization kinetics with special reference to fused silica. Phys. Chem. of Glasses **7**, 159–168 (1966)

Volarovich, M.P., Leontieva, A.A.: Determination of the viscosity of quartz glass within the softening range. Soc. Glass Technol. **20**, 139–143 (1936)

Wackerle, J.: Shock-wave compression of quartz. J. Appl. Phys. **33**, 922–937 (1962)

Walsh, J.M., Shreffler, R.G., Willig, F.J.: Limiting conditions for jet formation in high velocity collisions. J. Appl. Phys. **24**(3), 349–359 (1953)

Zoltai, T., Buerger, M.J.: The crystal structure of coesite, the dense, high-pressure form of silica. Z. Krist. **111**, 129–141 (1959)

Received February 8, 1976 / Accepted June 28, 1976